



UNIVERSITÀ
DEGLI STUDI
DI PADOVA

UNIVERSITA' DEGLI STUDI DI PADOVA

Dipartimento di Ingegneria Industriale DII
Department of Polymer Engineering

Corso di Laurea Magistrale in Ingegneria Meccanica

PA 12 composites with Graphite and MWCNT produced by SLS,
Injection Moulding and Compression Moulding: Performance analysis

Relatore

Prof. Giovanni Lucchetta

Relatore

Prof. António José Vilela Pontes

Correlatore

Dott.ssa Ana Carina Ferreira Lopes

Laureando

Emanuele Pozza 1185149

Anno Accademico 2019/2020

Abstract

PA12 composites with Graphite and MWCNT produced by SLS, Injection Moulding and Compression Moulding: Performance analysis

The continuous growth of Selective Laser Sintering (SLS) is closely linked to the development of ever new materials, able to get as close as possible to the results obtained with traditional manufacturing technologies such as Injection Moulding (IM) and Compression Moulding (CM).

Therefore, this study focused on the study of the influence of graphite and carbon nanotubes (CNTs) in a polymer matrix composite (PMC), in which polyamide 12 (PA12) was used as a matrix, producing samples with three different technologies, namely SLS, IM and CM. The main ratios studied were PA12 with 30% graphite, PA12 with 10% graphite and 3% CNTs, PA12 with 3% CNTs, PA12 with 10% graphite, PA12 with 0,8% CNTs. The specimens obtained were then subjected to mechanical, electrical, thermal and morphological tests.

The results of this research showed a real influence of graphite and CNTs on the final properties, although the electrical and thermal conductivity has undergone little improvement, not allowing to obtain sufficiently conductive materials. Despite this, graphite appears to be the best filler to add if the target are mechanical and thermal properties, while both fillers, or only CNTs, show a greater increase in electrical properties. Dispersion seems to be primarily responsible for these results, in light of the better results provided by IM and its intrinsic mixing.

Contents

| | |
|--|-----------|
| Abstract..... | i |
| Contents | iii |
| List of Figures | v |
| List of Tables..... | ix |
| List of Abbreviations and Symbols | xi |
| Chapter 1. Introduction..... | 1 |
| 1.1 Introduction..... | 2 |
| 1.2 Objectives | 4 |
| 1.3 Thesis organization..... | 4 |
| Chapter 2. State of the Art..... | 7 |
| 2.1 Selective Laser Sintering (SLS) | 8 |
| 2.1.1 Process description | 10 |
| 2.1.2 Process parameters | 11 |
| 2.1.3 Materials..... | 17 |
| 2.2 Injection Moulding (IM)..... | 18 |
| 2.2.1 Process description | 20 |
| 2.2.2 Process parameters | 22 |
| 2.3 Compression Moulding (CM) | 26 |
| 2.3.1 Process Description..... | 29 |
| 2.3.2 Process Parameters..... | 30 |
| 2.4 Composite materials for SLS, IM and CM | 31 |
| 2.4.1 Graphite-based composites | 37 |
| 2.4.2 Carbon Nanotubes-based composites..... | 39 |
| Chapter 3. Experimental component | 43 |

| | |
|--|-----------|
| 3.1 Methodology description | 44 |
| 3.2 Composite preparation..... | 44 |
| 3.3 Composite processing by Selective Laser Sintering..... | 45 |
| 3.4 Composite processing by Injection Moulding | 47 |
| 3.5 Composite processing by Compression Moulding..... | 49 |
| 3.6 Characterization tests | 52 |
| Chapter 4. Discussion of the Results | 55 |
| 4.1 General Consideration about the Manufacturing Processes..... | 56 |
| 4.2 Mechanical Properties | 58 |
| 4.3 Electrical Properties | 63 |
| 4.4 Thermal Properties | 67 |
| 4.5 Morphology Properties | 70 |
| Chapter 5. Conclusions and Future Work | 79 |
| 5.1 Conclusions and Future Work | 80 |
| References | 85 |
| Sommario | 93 |

List of Figures

| | |
|---|----|
| Figure 2.1 - Typical configuration of an SLS equipment (Adapted from [9]) | 8 |
| Figure 2.2 - Powder Deposition System (Adapted from [5]) | 9 |
| Figure 2.3 - SLS Process Sequence (Adapted from [9]) | 11 |
| Figure 2.4 - Powder Shape (Adapted from [5]) | 12 |
| Figure 2.5 - Packing Density [10] | 13 |
| Figure 2.6 - Injection moulding machine [17] | 19 |
| Figure 2.7 - Mould for IM (Adapted from [19]) | 20 |
| Figure 2.8 - Processing cycle of IM process (Adapted from [23]) | 20 |
| Figure 2.9 - Compression Moulding Machine [26] | 27 |
| Figure 2.10 - CM Mould Closures Type: (a) Positive; (b) Semipositive; (c) Flash (Adapted from [28]) | 28 |
| Figure 3.1 - SLS Dogbone Specimen Dimensions | 46 |
| Figure 3.2 - IM Dogbone Specimen Dimensions | 47 |
| Figure 3.3 - Mould Pressure and Mould Temperature versus Time in CM Process | 50 |
| Figure 3.4 - CM Dogbone Specimen Dimensions | 51 |
| Figure 4.1 - PA12 Sample with Black Point Produced by IM | 56 |
| Figure 4.2 - CM Die After Process | 57 |
| Figure 4.3 - Fracture Strength and Elongation at Break of IM Specimens with Different Amount of Graphite | 58 |
| Figure 4.4 - Yield Strength and Young's Modulus of IM Specimens with Different Amount of Graphite and CNTs | 59 |
| Figure 4.5 - Elongation at Break of IM Specimens with Different Amount of Graphite and CNTs | 60 |
| Figure 4.6 - Yield Strength and Young's Modulus of CM Specimens with Different Amount of Graphite and CNTs | 60 |
| Figure 4.7 - Yield Strength and Young's Modulus of SLS Specimens with Different Amount of Graphite and CNTs | 61 |
| Figure 4.8 - Yield Strength and Young's Modulus of pure PA12 Specimens using IM, CM and SLS | 61 |
| Figure 4.9 - Yield Strength and Young's Modulus of Composite Specimens using IM and CM | 62 |
| Figure 4.10 - Yield Strength of the Specimens | 62 |
| Figure 4.11 - Young's Modulus of the Specimens | 63 |

| | |
|--|----|
| Figure 4.12 - Elongation at break of the Specimens | 63 |
| Figure 4.13 - Electrical Conductivity of IM Specimens | 64 |
| Figure 4.14 - Electrical Conductivity of SLS Specimens | 65 |
| Figure 4.15 - Electrical Conductivity of CM Specimens | 65 |
| Figure 4.16 - Electrical Conductivity of Composite Specimens using IM and CM..... | 66 |
| Figure 4.17 - Electrical Conductivity of the Specimens | 66 |
| Figure 4.18 - Thermal Conductivity of IM Specimens | 68 |
| Figure 4.19 - Thermal Conductivity of CM Specimens..... | 68 |
| Figure 4.20 - Thermal Conductivity of SLS Specimens..... | 68 |
| Figure 4.21 - Thermal Conductivity of pure PA12 Specimens using IM, CM and SLS | 69 |
| Figure 4.22 - Thermal Conductivity of Composite Specimens using IM and CM..... | 69 |
| Figure 4.23 - Thermal Conductivity of the Specimens | 70 |
| Figure 4.24 - Transversal Section of IM Specimens (10x): I) Pure PA12; II) PA12 with 30% Graphite; III) PA12 with 10% Graphite and 3% CNTs; IV) PA12 with 3% CNTs | 71 |
| Figure 4.25 - Transversal Section of IM Specimens (4x): I) PA12 with 30% Graphite; II) PA12 with 10% Graphite and 3% CNTs; III) PA12 with 3% CNTs | 71 |
| Figure 4.26 - Transversal Section of CM Specimens (10x): I) Pure PA12; II) PA12 with 30% Graphite; III) PA12 with 10% Graphite and 3% CNTs; IV) PA12 with 3% CNTs | 72 |
| Figure 4.27 - Transversal Section of CM Specimens (4x): I) PA12 with 30% Graphite; II) PA12 with 10% Graphite and 3% CNTs; III) PA12 with 3% CNTs | 72 |
| Figure 4.28 - Transversal Section of PA12 with 10% Graphite and 3% CNTs Specimen by CM (4x) | 72 |
| Figure 4.29 - Transversal Section of SLS Specimens (10x): I) Pure PA12; II) PA12 with 10% Graphite; III) PA12 with 10% Graphite and 0.8% CNTs | 73 |
| Figure 4.30 - Transversal Section of SLS Specimens (4x): I) Pure PA12; II) PA12 with 10% Graphite; III) PA12 with 10% Graphite and 0.8% CNTs | 73 |
| Figure 4.31 - Transversal Section of PA12 Specimens (10x): I) IM; II) CM; III) SLS | 74 |
| Figure 4.32 - Transversal Section of PA12 with 30% Graphite Specimens (10x): I) IM; II) CM..... | 75 |
| Figure 4.33 - Transversal Section of PA12 with 30% Graphite Specimens (4x): I) IM; II) CM..... | 75 |
| Figure 4.34 - Transversal Section of PA12 with 10% Graphite and 3% CNTs Specimens (10x): I) IM; II) CM | 75 |
| Figure 4.35 - Transversal Section of PA12 with 10% Graphite and 3% CNTs Specimens (4x): I) IM; II) CM | 76 |
| Figure 4.36 - Transversal Section of PA12 with 3% CNTs Specimens (10x): I) IM; II) CM | 76 |

Figure 4.37 - Transversal Section of PA12 with 3% CNTs Specimens (4x): I) IM; II) CM76

Figure 4.38 - Transversal Section of Specimens through SEM (130x): I) PA12+10%Gr+3%CNTs by IM; II) PA12+10%Gr+3%CNTs by CM; III) PA12+10%Gr+0.8%CNTs by SLS77

Figure 4.39 - Transversal Section of Specimens through SEM (1000x): I) PA12+10%Gr+3%CNTs by IM; II) PA12+10%Gr+3%CNTs by CM; III) PA12+10%Gr+0.8%CNTs by SLS77

Figure 4.40 - Transversal Section of Specimens through SEM (15000x): I) PA12+10%Gr+3%CNTs by IM; II) PA12+10%Gr+3%CNTs by CM; III) PA12+10%Gr+0.8%CNTs by SLS78

List of Tables

| | |
|---|----|
| Table 2.1 - Example of PMCs in SLS | 33 |
| Table 2.2 - Example of PMCs in IM | 35 |
| Table 2.3 - Example of Graphite as Filler in PMCs | 38 |
| Table 2.4 - Example of CNTs as Filler in PMCs..... | 40 |
| Table 3.1 - IM Process Parameters..... | 48 |
| Table 3.2 - CM Process Parameters..... | 50 |
| Table 3.3 - Characterization Tests | 52 |

List of Abbreviations and Symbols

| <i>Abbreviation</i> | <i>Definition</i> |
|--------------------------------|--|
| 3D | Three-Dimensional |
| ABS | Acrylonitrile Butadiene Styrene |
| Al ₂ O ₃ | Aluminium Oxide |
| AM | Additive Manufacturing |
| BMC | Bulk Moulding Compound |
| CAD | Computer-Aided Design |
| CB | Carbon Black |
| CF | Carbon Fiber |
| CM | Compression Moulding |
| CNF | Carbon Nanofiber |
| CNT | Carbon Nanotube |
| DMC | Dough Moulding Compound |
| DSC | Differential Scanning Calorimetry |
| EG | Expanded Graphite |
| EVA | Ethylene-Vinyl Acetate |
| GF | Glass Fiber |
| GIC | Graphite Intercalated Compound |
| GMT | Glass Mat Reinforced Thermoplastics |
| GNP | Graphite Nanoplatelets |
| GO | Graphite Oxide |
| HA | Hydroxyapatite |
| HDPE | High-Density Polyethylene |
| HIPS | High-Impact Polystyrene |
| IM | Injection Moulding |
| LDPE | Low-Density Polyethylene |
| LFRT | Long Fiber Reinforced Thermoplastics |
| PP-g-MA | Maleic Anhydride Grafted Polypropylene |
| MWCNT | Multi-Walled Carbon Nanotube |

| | |
|-------|----------------------------------|
| NBR | Acrylonitrile Butadiene Rubber |
| PA | Polyamide |
| PANI | Polyaniline |
| PBT | Polybutylene Terephthalate |
| PC | Polycarbonate |
| PCL | Polycaprolactone |
| PDMS | Polydimethylsiloxane |
| PE | Polyethylene |
| PEDOT | Poly(3,4-ethylenedioxythiophene) |
| PEEK | Polyether Ether Ketone |
| PEG | Polyethylene Glycol |
| PEKK | Polyether Ketone Ketone |
| PEN | Polyethylene Naphthalate |
| PET | Polyethylene Terephthalate |
| PI | Polyimide |
| PLLA | Poly (L-Lactic Acid) |
| PMC | Polymer Matrix Composite |
| PMMA | Poly(Methyl Methacrylate) |
| POM | Polyoxymethylene |
| PP | Polypropylene |
| PPE | Poly(P-Phenylene Ether) |
| PPS | Polyphenylene Sulfide |
| PS | Polystyrene |
| PSU | Polysulfone |
| PTFE | Polytetrafluoroethylene |
| PU | Polyurethane |
| PVA | Poly(Vinyl Alcohol) |
| PVC | Polyvinyl chloride |
| PVDF | Polyvinylidene Difluoride |
| RH | Relative Humidity |
| SAN | Styrene Acrylonitrile Resin |
| SBR | Styrene-Butadiene Rubber |

| | |
|------------------|------------------------------|
| SEM | Scanning Electron Microscope |
| SiC | Silicon carbide |
| SiO ₂ | Silicon dioxide |
| SLS | Selective Laser Sintering |
| SMC | Sheet Moulding Compound |
| SR | Silicone rubber |
| STL | Stereolithography |
| SWCNT | Single-Walled Nanotube |
| TPV | Thermoplastic vulcanizate |
| UTS | Ultimate Tensile Strength |

Chapter 1. Introduction

The general aspects of this work are presented in this introductory chapter. The following pages provide a brief presentation of the research context, the motivation behind this choice, the main objectives and finally a brief explanation of the structure of the thesis.

1.1 Introduction

In recent decades, traditional manufacturing industries for plastic products have come up against the growing request for more tailored and personalized products, that the market has start to demand. However, this new wind was at odds with the main advantages of the most popular manufacturing technologies relating to plastics, which were basically the low cost for high volumes and standardization.

The growing need for this type of products has therefore met the exponential growth of a new branch of technologies called Additive Manufacturing, which has guaranteed greater freedom in relation to the complexity of the products manufactured. The ASTM F2792 International committee defined Additive Manufacturing (AM) as the "process of joining materials to make parts from 3D model data, usually layer upon layer, as opposed to subtractive manufacturing and formative manufacturing methodologies" [1].

While AM technologies have been around since the early 1980s, interest in this type of production technology has only increased in recent years due to the advances in machinery, materials and software, reducing costs and processes complexity and achieving parts with properties comparable to those produced with traditional processes. A further boost to this expanding world has come with the advent of Selective Laser Sintering (SLS), one of the most promising technologies for the future, given the achievement of exceptionally robust parts. This technology allows the production of a part from a 3D (Three-Dimensional) CAD (Computer-Aided Design) file, previously prepared into a layer data, according to the settings of the powder bed fusion process.

The SLS process essentially consists of a laser beam which has to sinter a thin layer of powder, promoting the solidification of the areas corresponding to the cross-section of the chosen geometry, inside a processing chamber with an inert and thermally controlled environment. The multiple repetition of this phase results in a three-dimensional solid polymer part, surrounded by the loose powder that has not be processed and can be reused.

Currently one of the main problem of SLS is the limited material selection, due to the need to find the combination of intrinsic and extrinsic properties of the material to obtain a powder suitable for the process. This limitation can also lead to the lack of final mechanical properties

of the parts, especially when compared with those produced by traditional manufacturing processes, such as Injection Moulding (IM) or Compression Moulding (CM).

Furthermore, since the powders used are mainly plastic powders, that are intrinsically insulating, the materials obviously lack good electrical and thermal properties, which could be useful in particular contexts, such as custom-moulded heat sinks for electronic devices or tubing for heat exchangers in various field of use.

Taking these needs in account, increasing materials availability would certainly lead to an important expansion of SLS technology in the AM plastics market, even replacing some traditional technologies thanks to the achievement of customized component with sufficient properties, although the costs of the entire process still remain high.

In this perspective, the idea of using fillers has become increasingly popular, thanks to the possibility of these materials to improve some important properties of plastic powder, such as mechanical strength, electrical and thermal conductivity. Composite materials, as the combination between a plastic and a filler is called, are already widely used today in many manufacturing processes to date, but their entry into the world of AM has only taken place in recent years. Their use can also expand the range of processing materials available, giving the manufacturer the possibility to use the best material for each particular situation.

The idea of using graphite and carbon nanotubes (CNT) was born from the knowledge of the well-known mechanical, electrical and thermal properties, that both can guarantee to the composite, combined, for the graphite, with the opportunity to reuse this material as production waste, ensuring reduced costs and sustainable practices, a very topical issue regarding polymeric materials. This advantageous recycling process could also be interesting in an attempt to reduce costs, which is one of the current problems of the SLS process.

Studying how these types of fillers influence the properties of pure material through SLS technology also seems useful to understand if their behavior differs from that obtained in conventional processes such as IM and CM. A further interesting topic to study is the way in which the two reinforcements interact with each other when they are both processed by SLS. This could lead to a better understanding to identify the best method to efficiently use fillers

Chapter 1. Introduction

and reinforcements in SLS, which can be totally different from what is established in traditional processes.

1.2 Objectives

In the context described so far, the objective of this work mainly concerns the attempt to obtain new composite materials for SLS capable of exceeding the performance of the currently most used material, Polyamide 12 (PA12), through the use of some type of reinforcements, i.e. graphite and carbon nanotubes, comparing the improvements provided by the same reinforcements in traditional manufacturing processes, namely Injection Moulding and Compression Moulding.

In consequence, to achieve this main goal, the general objectives of this dissertation are:

- a. Produce specimens with pure PA12 using SLS, IM and CM;
- b. Produce specimens with different mixture ratio of PA12 and graphite using SLS, IM and CM;
- c. Produce specimens with different mixture ratio of PA12 and CNT using SLS, IM and CM;
- d. Produce specimens with different mixture ratio of PA12, graphite and CNT using SLS, IM and CM;
- e. For a), b), c) and d), study specimens by dimensional, mechanical, electrical, thermal and microstructural tests.
- f. Evaluation of the influence of the fillers and the technologies on properties

1.3 Thesis organization

In order to have a well-defined work base to achieve all the proposed objectives, this thesis is divided into five main chapters.

The current, Chapter 1, provides a brief introduction to the field of research and the main objectives that this work intends to achieve in this context.

Chapter 2 reviews the state of art of each of the three manufacturing technologies used, namely Selective Laser Sintering, Injection Moulding and Compression Moulding, providing all the necessary theoretical explanations regarding the main stages of the process, machine components, parameters and most common materials used.

Chapter 3 focuses on the experimental components, in particular the working methods adopted, equipment, materials and process conditions are described in more detail. In this part there is also a summary with all the characterization tests carried out on the specimens, i.e. Evaluation of Mass and Dimensions Variation, Tensile Tests, Electrical Tests, Differential Scanning Calorimetry (DSC), Microstructural Test and Microscopical Evaluation (SEM), including the corresponding test conditions.

Chapter 4 analyses all the results of the experimental tests in order to discuss whether the objectives have been achieved or not, through multiple comparisons between the different technologies and the different mixing ratios considered and tested.

Chapter 5 presents a complete final report of this work, combining them to the conclusions that have been reached through an in-depth analysis. There are also some possible ways to apply the results in future work.

Chapter 1. Introduction

Chapter 2. State of the Art

This chapter presents and explains the most important knowledge to understand the research. In particular, this second chapter provide some general information on IM, CM and especially on SLS. For each technology there are a brief review of the history of the technology, an explanation about the main components of a typical machine, a simple overview over the process, together with a description of the main parameters that influence the process. In the end, a brief summary of the main composite materials is presented, focusing on the carbon-based ones used in this work.

2.1 Selective Laser Sintering (SLS)

During the 1980s, at University of Texas at Austin, a mechanical engineering undergraduate and an assistant professor developed a new AM technology that used for the first-time discrete particle, i.e. the powder, and that would become one of the most promising manufacturing methods nowadays [2] [3]. A lot of different machines have been developed starting from their initial idea, in order to increase the productivity, increase the materials choice and avoids the process' intrinsic weakness [4]. However, all the derivate processes share the same basic characteristics: an enclosed chamber, some heaters, one or two feed powder reservoirs (on one side or on both), a device to add and smooth the powder layer, a construction platform system, a laser and an optical correction system (Figure 2.1) [3][4].

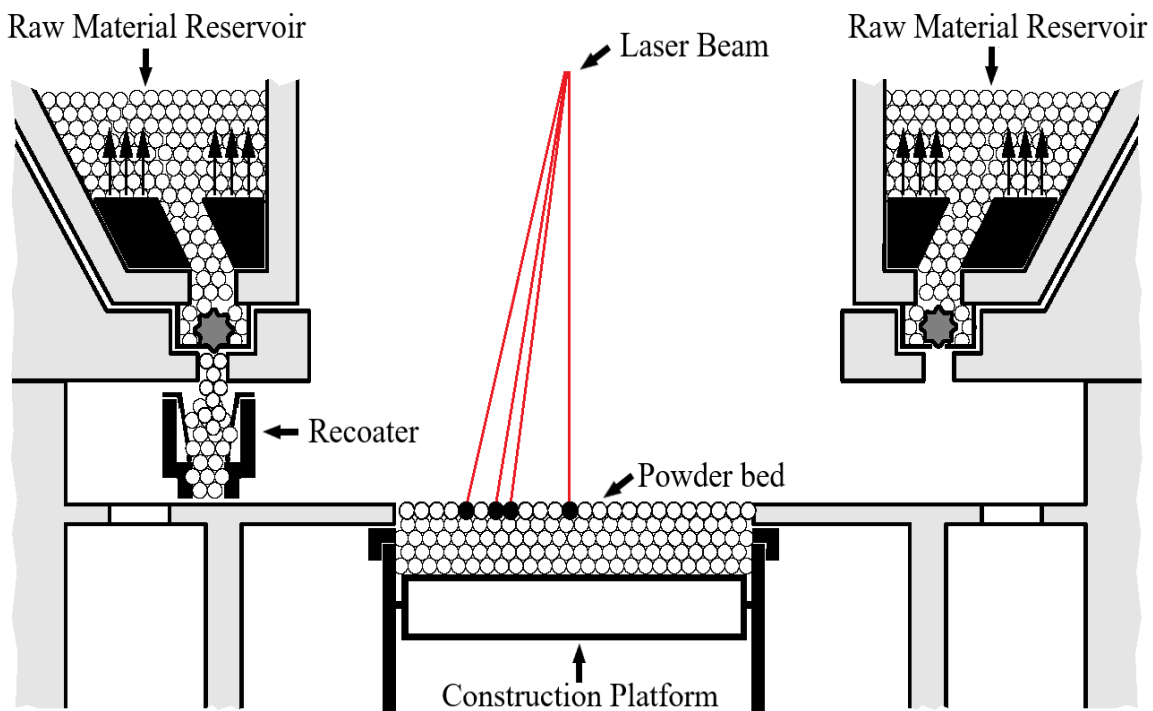


Figure 2.1 - Typical configuration of an SLS equipment (Adapted from [9])

The closed chamber is where the part building process takes place and it is characterized by the presence of nitrogen gas in order to minimize oxidation and degradation of the material [4].

Just above the construction platform, inside the building chamber, there are some infrared heaters positioned to ensure that the temperature remains just below the melting temperature and/or the glass transition temperature, depending on the material. Some other heaters are also positioned above the feed reservoirs to pre-heat the powder before spreading it over the build area [3][4]. The objectives of these pre-heating and maintenance processes are to minimize the laser power requirements and to prevent warping effects due to non-uniform thermal expansion and contraction [4].

The two feed reservoirs are necessary to deliver the raw material to a recoater, or a simple roller/blade, which has the task of spreading it and smoothing it over the whole powder bed (Figure 2.2) [3][4].

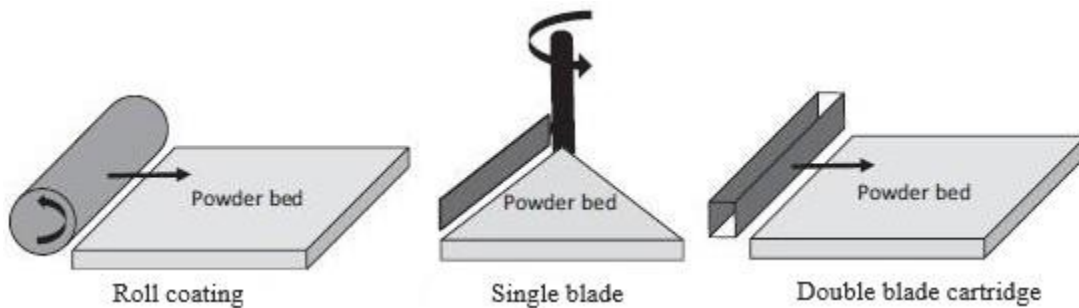


Figure 2.2 - Powder Deposition System (Adapted from [5])

The construction platform, as the name suggests, is the place where the part is built. The platform can be raised or lowered to create a new layer of powder at each cycle [4].

Last but not least, the essential optical components in a SLS process are the laser, the laser beam guide and the scan head [5]. The laser has to provide enough heat to selective sinter the powder [3]. The laser beam guide and the scan head consist of some mirrors whose objectives are to guide and to focusing the laser to the chosen path on the powder bed, to follow the previous CAD model [3][5].

2.1.1 Process description

The SLS process starts with the introduction of the powder material inside the reservoirs within the thermally and atmospherically controlled closed chamber [5].

The following fundamental step concerns the preheating of the chamber and the powder to the process temperature, which has to be reached and maintained elevated and uniform. This initial warm-up is really important, and it could take hours [5]. When the system reaches the right temperature, the reservoir supplies a certain amount of material to the recoater, or directly to the powder bed, which is spread across the whole bed to form a thin layer [4].

A focused CO_2 laser beam is then directed onto the powder bed where the material is selectively sintered to form the sliced cross-section, according to the model design [3][4]. This sintering process occurs due to physical-chemical transformation phenomena [3].

The surrounding powder, that remains unchanged by the sintering process, acts as natural support for the subsequent layers and it has to be removed after the end of the process. The remaining powder can be reused in another process [3][4].

After a short-term cooling down phase to avoid excessive internal stress, it is possible to lower the build platform by a layer thickness in order to free up space for the subsequent powder deposition [3][4][7].

This process is then repeated until the whole part has been built, in a bottom-up process [3].

After the entire part has been sintered, a slow and controlled cooling down of the part is typically required to allow the part to uniformly reach a low-enough temperature to be handled and exposed to the atmosphere. If the product is prematurely exposed to room temperature, it may suffer oxidation and warpage effects due to an uneven thermal contraction [3][4][5]. This cooling phase takes a long time, theoretically the same time necessary to build the part, followed a rule of thumb, but in practice it's 1.5 times or even more [5].

Finally, after the end of the cooling phase, the construction platform is raised to its starting position. At that moment the part can be removed from the powder bed, the loose powder is

cleaned off and, if necessary, further finishing operations are carried out, such as sanding or painting [3][4]. Figure 2.3 generally represents the SLS process previously described.

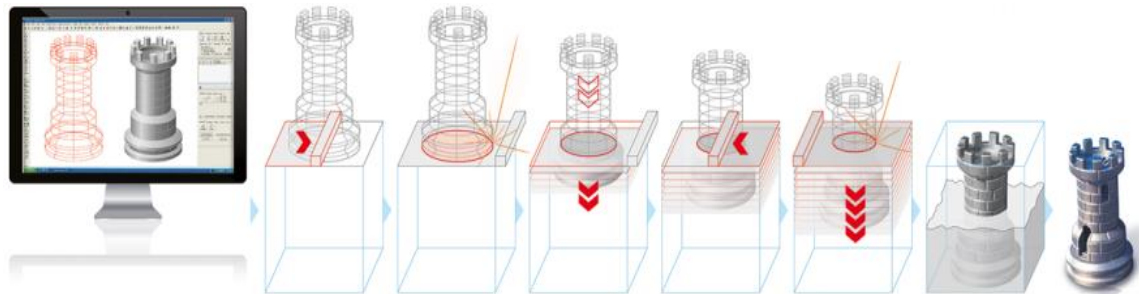


Figure 2.3 - SLS Process Sequence (Adapted from [9])

2.1.2 Process parameters

The SLS process includes a large number of different parameters, many of which are strongly interdependent and mutually interacting, generating a complex scenario of choices that determine the outcome of the process [3][4]. These parameters can be lumped into five categories: powder-related parameters (e.g. shape, density, size and distribution, layer thickness, material properties), laser-related parameters (e.g. laser power, spot size, pulse duration, pulse frequency, beam offset), temperature-related parameters (e.g. powder bed temperature, powder feeder temperature, temperature uniformity), scan-related parameters (e.g. number of scans, scan speed, scan spacing and scan pattern) and part-related parameters (e.g. part position, part orientation) [3][4].

Powder Parameters

The parameters related to the powder can be divided in two further group: intrinsic (thermal, rheological and optical) and extrinsic (particles and powder). The intrinsic parameters are related to the molecular structure of the polymer itself, and therefore they are difficult to influence, while the extrinsic ones, since they are determined by manufacturing or by

Chapter 2. State of the Art

previous processes, can be more easily controlled and they have a strong impact on the absorption characteristics, on the powder bed density and on the power spreading [3][4][10].

The shape, together with the surface, has a strong influence on the powder behaviour during the SLS process, leading to an inhomogeneous powder bed if the particles are not largely round and the surface is very rugged and chopped. The shape of the powder particles is essentially determined by the manufacturing process, where usually three different common shapes are obtained: spherical, potato-shaped and edged (Figure 2.4) [5]. This vital variable influences the fluidity, since it is necessary to obtain a suitable powder flowing behaviour, the density, the surface roughness and the final porosity of the part [3][10]. As for the porosity, it tends to be greater on the surface of the layer than inside the part and in addition it increases with the decrease in laser energy due to an incomplete fusion [3]. This problem is even more accentuated if the ratio between layer thickness and average particle size decrease [10]. Moreover, the larger irregular voids, generated by the shape, determine a weak elongation at break of the part [3].

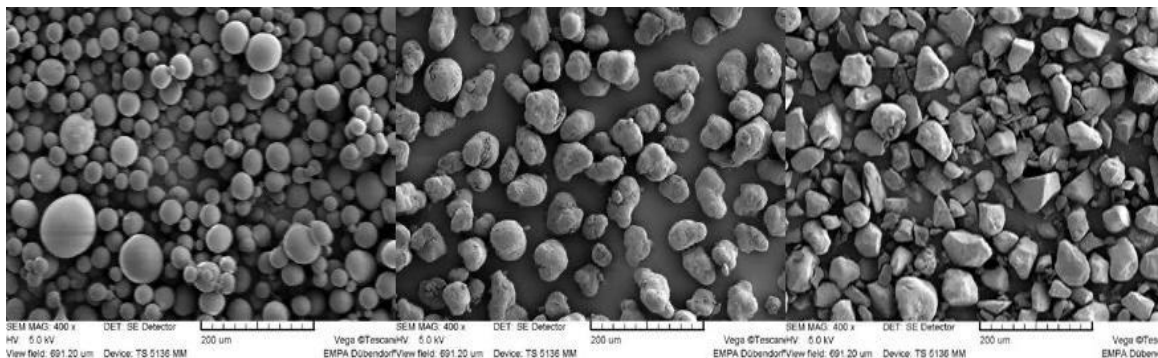


Figure 2.4 - Powder Shape (Adapted from [5])

As regards the relationship between shape and density, the increase in roundness also involve an increase in packing density [3]. Theoretically, the best possible arrangement for the powder would consist of spherical shapes in order to occupy the widest possible space (Figure 2.5). The only possible way to increase the density would be to fill the interstices between the powder with smaller particles without expanding the overall volume [3][5]. This idealized disposition is not reflected in the real process, due to the random deposition process,

the lack of perfect spherical shapes and the poor dispersion of small particles that increase the overall volume [3].

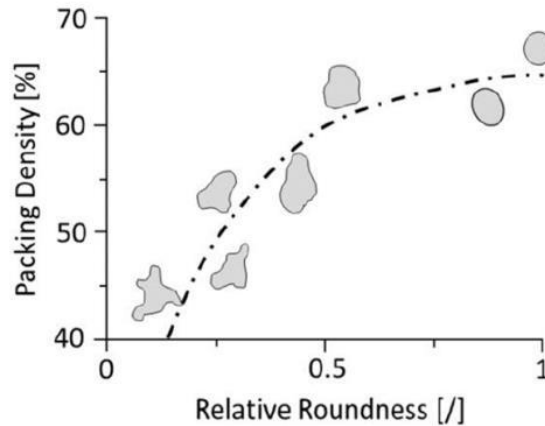


Figure 2.5 - Packing Density [10]

The SLS powders currently available on the market have a density in the range between 45 and 50%, reaching about 60% for technical applications [5].

In general, the increase in density can lead to an improvement in mechanical properties, due to the contemporaneous decrease in shrinkage and distortion, a denser sintered part and a better stability of the powder bed [3][10]. On the contrary, the decrease of this important parameter could bring to a worse material deposition, that can lead to an inhomogeneous part, the formation of some massive cavities and an irregular surface structure [5].

The density is also closely related to the molecular weight of the polymer, one of the most important factors among the material properties [4]. To guarantee an adequate value of the melting density it is essential to maintain a molecular weight low enough to allow the material to fill the interparticle gaps to provide particle adhesiveness, but high enough to not let the polymer sink into the powder bed to avoid obtaining porosity [3]. This property is not so easily controllable both during polymer production and during the process. An increase in molecular weight can achieve functionally stronger parts, better flowability, less shrinkage, and therefore better dimensional accuracy, but also a more difficult spreading on the powder bed due to the higher viscosities [3].

Chapter 2. State of the Art

Another important parameter of SLS process is the powder size, which, as well as its distribution, has a decisive influence on powder behaviour, or rather on laser absorption characteristics, powder bed density and powder spreading [4][5]. The size of the powder comes directly from the adopted manufacturing system [3].

Smaller particles can lead to more efficient laser energy absorption, lower porosity, a smoother surface, better resolution, thinner layers and more flowability, while at the same time leading to a more difficult spreading on the build platform and even a poor laser-powder interaction if the size falls below the laser wavelength [3][4].

On the other hand, larger particles are more difficult to melt due to the material's poor thermal diffusivity, which causes more porosity and rougher surfaces on the parts [3].

Having to choose a compromise solution, the ideal size of the powder is generally considered between 45 and 90 μm , an interval that can avoid most agglomerates problems and also the triboelectric loading problem [3]. The maximum size is however limited by the minimum layer thickness, which is normally between 60 and 160 μm , where the average particle diameter is between 30 and 60% of the layer thickness [10].

It is necessary to find an optimal compromise also with regards to the layer thickness, the parameter that actually control the processing time, and therefore the final cost of the sintered part. As a matter of fact, if a decrease in layer thickness can lead to a faster process and also to a decrease in the maximum value of the crystallization, on the other hand it leads to a series of problems such as poor sintering, due to the low powder bed density, the stair stepping problem and rougher surfaces [3][10].

Normally the layer thickness is at least twice the average size of the powder, so that the fusion can take place by direct fusion of the material and not through conduction between particles [3]. The range in which the thickness is usually positioned is between 0.1 and 0.15 mm [4][5].

Laser/Temperature Parameters

The two most important parameters related to laser and temperature, respectively, the laser power and the bed temperature, are mutually interdependent and they should be balanced, with the contribution of scan speed and scan spacing, to provide the best trade-off between dimensional accuracy, surface finish, build rate and mechanical properties [3][4]. Using a high laser power value and a high bed temperature, the final part can become denser, improving the mechanical properties, but at the same time it can create problems like partial growth, difficulties in recycling and part cleaning [3]. At the opposite end, keeping both values low can bring to better dimensional accuracy, but also to a decrease in density and a greater tendency to layer delamination. High laser power and low bed temperature instead cause an increased non-uniform shrinkage and a greater residual stress, leading to an increase in final curling [4].

In general, an increase in laser power results in more heating, which leads to greater strength, but also to an irregular shape and some curling on the surface [3]. On the other hand, by lowering the laser power it is also necessary to reduce the scan speed, to guarantee a proper particles fusion. This procedure guarantees better mechanical properties at the expense of productivity [4].

Usually the required laser power increases with the melting point of the material and with the lowering of the bed temperature, as well as with the absorptivity of the powder bed [4][5].

As for the bed temperature, it is generally set as high as possible but always below the melting temperature of the material (about 3-4°C) for semi-crystalline polymers [3].

Increasing this parameter allows the use of a lower value of laser power which also involves a reduction in the scan speed, with a consequent decrease in productivity. Raising it too much results in problems like unwanted binding or excessive compacted powder [3]. On the other hand, a decrease in the bed temperature can lead to a slow recrystallization, which is a good thing for the final result, but an excessive reduction causes a worsening of the mechanical properties and a non-uniform fusion that cause the increase of the porosity [3][4].

Chapter 2. State of the Art

A good choice of bed temperature can therefore guarantee a proper sintering process, since it influences the depth of the thermal energy, which is fundamental to increase the packing of the material and consequently it can improve the final mechanical properties [3][7].

The spot size, together with the laser power, the scan speed and the bed temperature, influences the energy input needed to properly sinter the powder particles, the sintering depth and the melt pool size [4][7].

Scan Parameters

Scan speed is the velocity of the laser movement across the bed surface during the sintering of the powder [8]. It is the parameter that has the greatest influence on the part build time, and therefore on the productivity of the process, and nowadays, among industries, there is the tendency to increase this speed to obtain greater profits [5]. To pursue this goal, the necessary increase in scan speed also requires an increase in laser power to ensure sufficient sintering [4].

On the other hand, the reduction of this parameter, together with a lower laser power, leads to improve the mechanical properties and reduce balling, a phenomenon in which there is the formation of small spheres about the size of the laser beam [3][7]. The most important problem concerning the use of a low value of the scan speed is the presence of the conductive heating between particles instead of the direct heating by the laser beam. To avoid this phenomenon, it is necessary to choose the right scan speed [3].

Another important parameter is the scan spacing, which represents the distance between two consecutive parallel laser scans. Together with layer thickness, it has a strong influence on the final part density, on the build speed and on the mechanical properties [3][4]. Scan spacing has to be chosen from a compromise between a high value, which leads to an increase in the laser power and therefore to oversintering, and a low value, which leads to an incomplete sintered cross-section and, consequently, a poor packing of the particles in the powder bed [3].

Part Parameters

Part build orientation is an important parameter of SLS process which represents the orientation of the major axis of the part with respect to the powder bed [11]. This parameter has a strong influence on the final quality of the surface, on the stair stepping effect, on the accuracy of the part details and, last but not least, on build time and therefore on costs [3].

One of the things to remember is that the materials fail more easily along the build direction due to the weak interlayer bonds. According to Veryst, the orientation to obtain the best properties is around 60° [3].

Anisotropy plays an important role when it is come to decide the orientation of the part, because it greatly influences the final mechanical properties. This eventually becomes an advantage, because it is possible to change the orientation based on specific geometric factors [5].

In general, it is also important to keep in mind that the build height is proportional to the build time and the needed powder in the process, and, therefore, to the costs of the process [3].

As for another important parameter, i.e. part position, it has a strong influence on the final shrinkage of the part due to the fact that the dimensional variation is not constant in the entire building area due to SLS intrinsically thermal gradients [3].

2.1.3 Materials

One of the qualities for which the process initially gained popularity was due to the large quantity of materials available, since practically any substance that can be pulverized into a fine powder can be used in the SLS process [6]. The first materials used were polymers, in particular polycarbonate (PC), polyvinyl chloride (PVC), polybutylene terephthalate (PBT) and polyamides (PA), mainly because they were already available as powders [5]. Subsequently this process was also extended to metals and ceramics [4][7].

Chapter 2. State of the Art

Currently, the most used materials are thermoplastic polymers, due to their low thermal conductivities, relatively low melting temperature, low tendency to show the balling phenomenon and ease of production [3]. Among these types of polymers, the ones that leads the grow of the SLS technology are certainly polyamides, and in general the use of semi-crystalline material instead of amorphous ones [5]. Semi-crystalline polymers guarantee better mechanical properties, better surfaces and higher densities, but they also bring more shrinkage, more curling and more distortion which have to be controlled to obtain accurate final products [3][4]. Due to the shrinkage it is essential that the melting temperature of the material is sufficiently higher than the crystallization temperature, or that the sintering window is quite large, to delay the crystallization and to have a more homogeneous microstructure between layers [3].

Today the SLS market is substantially covered by PA12 and PA11 and their derivatives, with over 95% of the total parts produced by PA12 and PA12 powder-based mixtures [5][12]. The reasons for this situation lie in the difficulty of finding new powders that at the same time obtain excellent intrinsic properties (e.g. sintering window, melt viscosity) and extrinsic (e.g. powder shape and surface), specific requirements to obtain a powder suitable for a successful process [3][12].

2.2 Injection Moulding (IM)

Injection moulding process date back to 1872, when the Hyatt brothers introduced the first example of an injection moulding machine, consisting of a simple plunger to inject the plastic through a heated cylinder into a mould [13]. Their device used cellulose, considered the first man-made thermoplastic.

The following success of IM took place during the 1940s, due to the demand created by World War II for inexpensive and mass-produced products [14].

In 1946, the primitive machine created by the Hyatt brothers was replaced by the new screw injection machine that would revolutionize the plastic world. His inventor, named James Hendry, foresaw the great potential that his idea would bring to the plastic world, mostly

because of the addition of a mixing phase and the reduction of energy thank of friction's additional heat [14].

Following Hendry's idea, a lot of developments were introduced with as objectives an improvement of products' quality and a time's reduction. Nowadays, many different types of IM machine can be built according to the unique need of the final product, such as injection-compression moulding or gas-assisted injection moulding [15]. The major components of an IM machine, as shown in Figure 2.6, are the injection unit, the clamping unit and the mould [16].

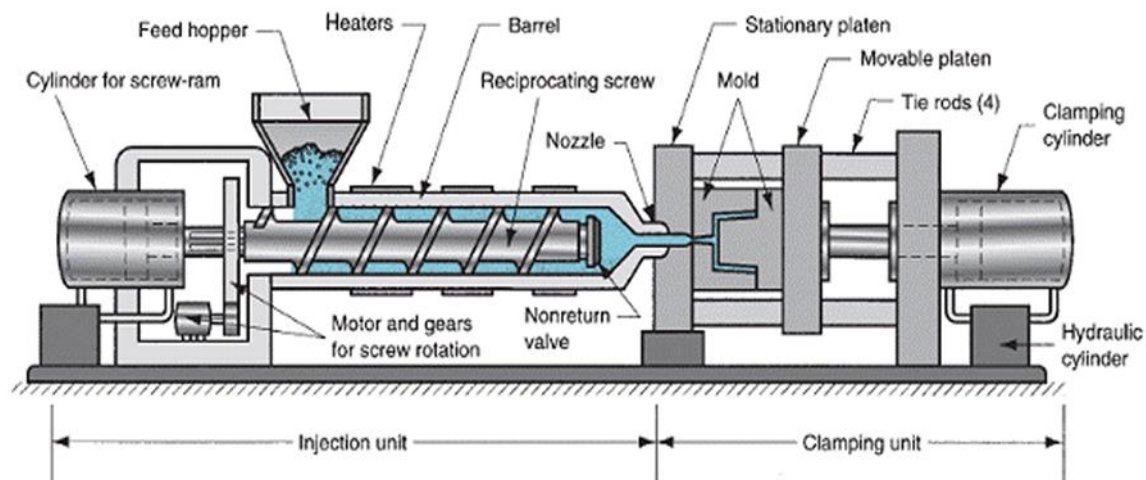


Figure 2.6 - Injection moulding machine [17]

The injection unit, also called plasticating unit, has the main tasks to melt the plastic material, to inject it into the mould and to maintain the hold pressure during cooling. It is usually composed of a hopper, a screw, a barrel, a handling system, some heater bands, a non-return valve and a nozzle. The screw can both rotate, to melt the plastic material with the heat due to friction, and translate, to inject the melted material [15] [16].

The clamping unit is used mainly to close and open the mould, and to counteract the injection pressure due to the injected material.

Last but not least, the mould is the key factor of an IM process (Figure 2.7). It has to distribute the melted material into the cavities, shape the part, cool the melt and eject the finished

Chapter 2. State of the Art

moulded product. The mould is basically custom-made, and it is usually composed of a runner system, a gate, some cavities, a cooling system and an ejector system [16]. A lot of different type of mould was introduced due to the necessity of high productivity, such as hot runner mould, three-plate mould or stack mould [18]. Despite being more complex, they guarantee high products' volume with low prices.

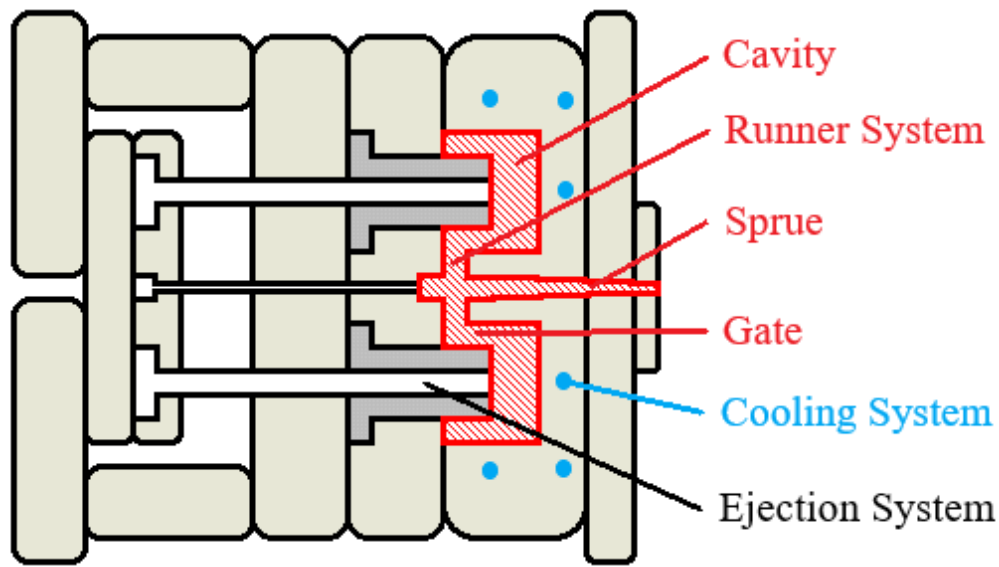


Figure 2.7 - Mould for IM (Adapted from [19])

2.2.1 Process description

The injection moulding process requires a lot of steps, but usually a whole cycle takes a few minutes at most. The process can change based on different kind of IM, but all retain the same origin (Figure 2.8).

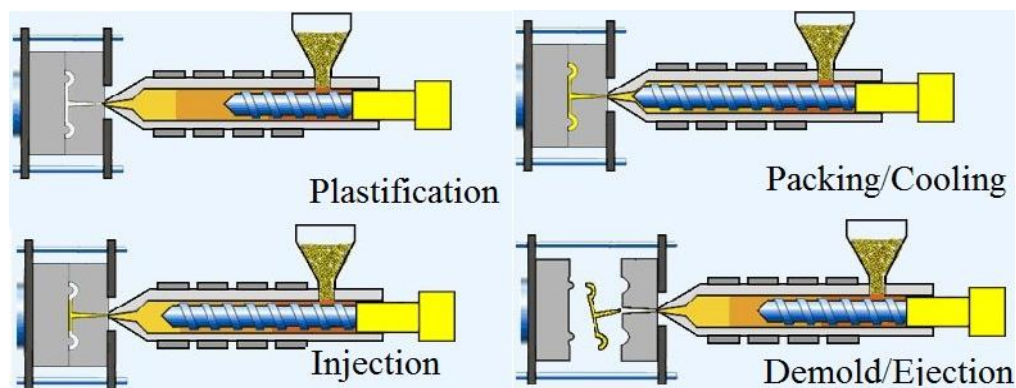


Figure 2.8 - Processing cycle of IM process (Adapted from [23])

The first work to do is to fill the hopper with the material, which is usually used in a pellet shape or, less commonly, as powder [15]. In the industrial field, the polymer is transported directly from the storage to the hopper by an automatic and closed system, due to humidity problem. This kind of material is indeed very sensible to little change of moisture content, a brief time in touch with environment could lead to huge change of material's characteristics, so much that this problem requires usually the utilization of a dehumidifier [20][21][22].

When the hopper is filled up, the screw starts to rotate to melt the material, using the heat from the heated barrel and from the internal viscous heating [18]. Some heaters bands are used to control the melt temperature, i.e. the temperature of the polymer inside the barrel, and to decide the temperature progression that the material has to go through [15].

The plasticized melt is therefore pushed forward, by the rotation, into the barrel's final chamber and at the same time the screw retreats axially due to the increasing volume in front of it. The screw slides back until there is the right size of material to fill the cavity and to compensate the following thermal contraction inside the mould. During the backward rotation, the screw receives a specific amount of pressure by the piston behind it, called back pressure, that reduce the return speed, homogenise better the polymer and increase the density [14][15].

After reaching the right amount of material, the rotation is stopped, and the entire plasticizing unit moves forward axially to bring the nozzle and the mould feeding bush into contact. This movement is necessary because these two parts touch each other only during the fill time, so as not to alter their respective temperatures [15].

A fundamental movement before the injection phase is the closing of the mould. The objective of this action is to form the cavity, usually made by two halves, and to guarantee a sufficient clamping force, or rather the force that has to be transmitted to the mould to ensure that it does not open due to the injection pressure [14][15].

Subsequent, the screw works as a hydraulic piston and it proceeds to move forward, only axially, to inject the molten material into the mould. At the end of the initial injection stroke, a so-called packing phase begins, and during this period the screw continues to inject additional polymer with a fixed pressure. This packing action is necessary due to the

Chapter 2. State of the Art

volumetric shrinkage of the injected material inside the mould and it provides a higher final density [14][15][18].

The moment in which the nozzle freezes marks the finish of packing and the beginning of the cooling phase, in which the cooling system inside the mould has to solidify the final product and to make it rigid enough to be extracted. Only after having reached these conditions, it is possible to open the mould and to push the final object out of the mould. Usually this task is performed by the ejection system: an ejection plate, in contact with the ejectors, is moved forward to make every ejector push the material simultaneously. After the return of the ejection plate, the injection machine is ready to start the next cycle [15][18].

2.2.2 Process parameters

Injection moulding process is characterized by a lot of parameters, according to a study more than 200, which affect directly or indirectly the outcomes. This is one of the biggest problems in IM due to the difficulty of finding the effect of one parameter on another [14].

Despite the abundance of variables, it is possible to group together the main parameters in four basic categories: temperature (e.g. melt temperature, mould temperature), pressure (e.g. injection pressure, hold pressure, back pressure, clamping force), time (e.g. cycle time, injection hold time, cooling time) and distance (e.g. shot size, cushion), sorted respectively for importance [14].

Temperature parameters

One of the most important factors is the melt temperature, i.e. the material's temperature throughout the flow path, that needs to be checked along the entire flow path. The reason behind this choice lies in this parameter's influence on the plastic's viscosity, considered the key rheological property in filling, due to the indirect correlation between them in which a temperature's increase leads to a viscosity's decrease [16][20]. Viscosity, and therefore melt temperature, conditions the material's 'flowability' into the mould, leading to problems like short shot, high fill pressure on one side and flash, bubbles or burns on the other [20][22]. It

is equally important to keep the temperature in the correct range to avoid problems even inside the barrel itself, such as polymer degradation or unmelted particles [24].

It is possible to control the melt temperature inside the barrel in an excellent way by using the main factors that control it, i.e. screw rotation speed, back pressure and the bands heaters' external heat [20][24]. Normally most of the heat comes from the shear heating, due to the screw rotation, and the main aim of band heaters is to provide the last third to ensure a better control on the melt temperature [14][20]. The temperatures of the different barrel's sections can be chosen based on the mechanism of material melting and conveying behaviours [24].

Another important parameter of injection moulding process is the mould temperature. This second temperature is controlled by a cooling system, in which a fluid, normally water, flows to guarantee a stable mould temperature during the cycle. The purpose of the cooling system is to lower the temperature of the plastic inside the mould until the material's solidification, i.e. to reach the ejection temperature at which it is possible to extract the final product [14]. The mould temperature control is significant because it influences many factors, such as cycle time, surface quality, shrinkage and crystallization [14][24].

Pressure parameters

Pressure plays a key role in the injection machine, and it is possible to identify two main areas that require pressure control: the injection unit and the clamping unit. These two sections have to develop pressure to oppose to each other, because the first one has to push the molten material into the mould and the other has to prevent opening of the mould [14].

Regarding the injection unit, the first pressure that is applied to the molten plastic is called injection pressure and it is developed by the main screw movement system which pushes the end of the screw to move the material inside the mould [14].

The injection pressure used depends on the plastic's melt flow characteristic and the required cavity pressure, since the material has to possess enough pressure to overcome the pressure drops first in the barrel and then through the nozzle, the runner system and finally the cavity. Ensuring the right pressure in the cavity is important to produce uniform products, since

Chapter 2. State of the Art

choosing the wrong value can lead to many problems such as short shot, flash, poor surface finish, warpage, sticking in cavity, etc. [20].

At the end of the filling phase, the injection mould machine has to apply another pressure, called hold pressure, whose tasks are to complete the last part of the filling and to continue to inject material to compensate for thermal contraction of the melt [15][20]. In this operation a cushion, i.e. a certain additional amount of material after the required shot, is needed to transfer the pressure from the barrel to the cavity and it provides also the material to make up to the shrinkage [14][20].

The hold pressure is normally controlled through a profile, generally consisting of 3 or 4 stages, that has to be adjusted according to the material, the mould and other parameters [24]. The profile's objective is to minimize the warpage and the shrinkage of the product, as well as avoiding many defects such as poor surface finish, void, flash, etc. [15][20].

Another important parameter of injection moulding process is the back pressure, i.e. the pressure generated on the shank of the screw by an external applied force, necessary to reduce the screw speed backward and to obtain a better melt's homogenization [20][24]. The back pressure starts to work right after the finish of the holding phase, when the screw starts to rotate to move forward the required material for the next cycle [14].

The main objectives of the back pressure reside in a better density, which affects the weight of the final product, in a better mixing, which improves the homogeneity of the melt, and in a further temperature increase [14][20]. Some common problems related to a wrong choice of this parameter can be voids, degradation (in particular with heat-sensitive and shear-rate-insensitive materials), bubbles, sink, etc. [22].

Regarding the clamp unit, the main parameter is the clamp force which has to keep the mould closed against the force generated by the material during injection and holding phases [14][20]. The clamp force applied, which is transformed into a clamp pressure, has to overcome the injection pressure to avoid the mould opening and the problems related to it, such as short shot, flash and non-uniform venting [14][15][22]. A low value of clamp force also leads to not being able to completely control the pressure parameters for possible adjustments. On the other hand, excessively increasing the clamp force can damage the

mould and the press, which have limited strength, as well as requiring a more powerful machine [14].

The clamp force is also important because its value is used to categorize the machine sizes, together with another value connected in turn to the maximum injection pressure and the maximum shot volume [15].

Time parameters

The parameter that sums up the time required for each activity between a cycle and the next one is called overall cycle time and it measures how long it takes to mould a single set of products [14]. Usually a regular cycle requires from fractions of seconds to minutes, depending on shot size and/or wall thicknesses [20]. The main contributions come from the hold time and especially the cooling time, while the injection time does not have too much influence [15].

The cycle time is mainly used to study the impact of the manufacturing process onto the final cost of the product and reducing this time is the easiest way to reduce even the price [3]. To lower this overall time, a solution could be a more accurate control over the entire injection moulding process [20].

Within the overall cycle time, one of the most important part is the hold time, which defines how much time the screw has to maintain a certain amount of pressure against the plastic injected into the mould [14]. The holding phase is possible as long as the gate freezes, therefore the hold time is superiorly limited by reaching this point [14]. To find an optimum hold time usually it's possible to measure the part weight to reach a maximum, which has great influence on quality and productivity [20][24].

The longest time required in the overall cycle time, up to 80%, is the time used for cooling, in which the cooling system need to lower the plastic's temperature in order to let the material reach the mould release temperature, also called ejection temperature [14][20][24]. Once this temperature is reached, the part can be ejected avoiding breaks or pin pushes [22].

Chapter 2. State of the Art

The cooling time has a strong impact on productivity, and therefore on costs too, so an attempt is made to keep it as low as possible, considering that the minimum cooling time is governed by the wall thickness of the mould, by the difference between melt temperature and mould temperature and by the difference between ejection temperature and mould temperature. It is usually possible to estimate the minimum cooling time with some simple equations, in which most of the time it is directly proportional to the square of the thickness [20].

Many times, in companies there is the custom of setting a longer cooling time, in order to avoid warpage outside the mould [20][22]. The extension of the cooling time certainly allows to obtain more volumetric shrinkage, a part stiffer and a lower part temperature, but on the other hand it leads to a reduction in productivity, to an excessive in-mould shrinkage and to higher necessary ejection forces [18][22].

Distance parameters

The shot size is the amount of material that accumulates in front of the screw and which is injected into the mould during a single injection stroke [20]. The shot size is chosen based on the material needed to completely fill the cavities and all the runner system and to compensate the internal shrinkage of the part [20]. This parameter is really important due to the influence on the melt temperature, with the consequent risk of material degradation. Mistaking the value of the shot size can lead to many problems, such as short shots, voids, different densities, flow lines and many other problems [24].

2.3 Compression Moulding (CM)

Compression moulding is one of the oldest material processing methods, as well as the main manufacturing technology for plastic in the first half of the twentieth century, reaching up to 70wt% of all plastics. The reason for this dominance was the development of a phenolic resin in 1909, the wide use of which contributed greatly to the expansion of the CM process [25][26].

The use of CM began to decrease with the development of thermoplastic materials, which from the 1940s contributed to the great expansion of extrusion and above all of injection moulding. The increasing use of these new materials contributed to reducing the quantity of plastics processed by CM, leading to a share of its use of less than 25%, which continued to decrease up to 3% at the end of the century, while at the same time the use of thermosets went from 95wt% in the early 1900s, to 15% by the end of the century. The reason behind this decline lies in the intrinsic characteristics of the process, which make it more suitable for the processing of thermosetting materials, while it is rarely used with thermoplastics [25].

Despite being present for over a hundred year, a basic CM machine is composed by a common set of components, which are represented in Figure 2.9.

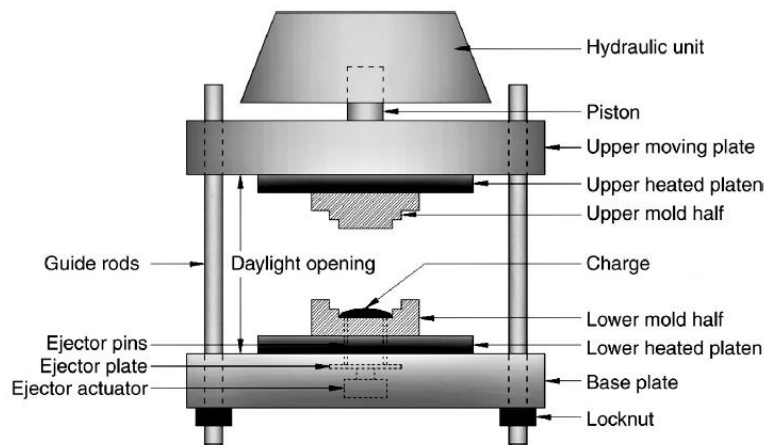


Figure 2.9 - Compression Moulding Machine [26]

The main components of the machine can be divided into two sections: the main element of the lower section consists of a robust metal base plate, which has to support a lower platen and four guide rods. The lower platen has the tasks of supporting and directly heating/cooling the lower half of the mould, while the four guide rods allow the upper plate to go up and down. A part ejection system, consisting of ejection pins connected to a plate, may be part of the lower mould or integral to the plate system [26].

The upper section of the machine consists of a movable upper plate and a hydraulic unit. The upper plate, like the lower plate, has to support the upper heated platen, which in turn has to support the upper half of the mould, in addition to having to heat/cool it. The hydraulic unit, which consists of a hydraulic-powered piston, has the task of forcing the platen system

Chapter 2. State of the Art

downward to perform compression. This type of compression press is called downstroke machine, in opposition to the upstroke machine, in which the hydraulic force is upwards [26].

As for the mould, there are three formal types of mould closures, as can be seen in Figure 2.10, differentiated according to the quantity of flash they produce.

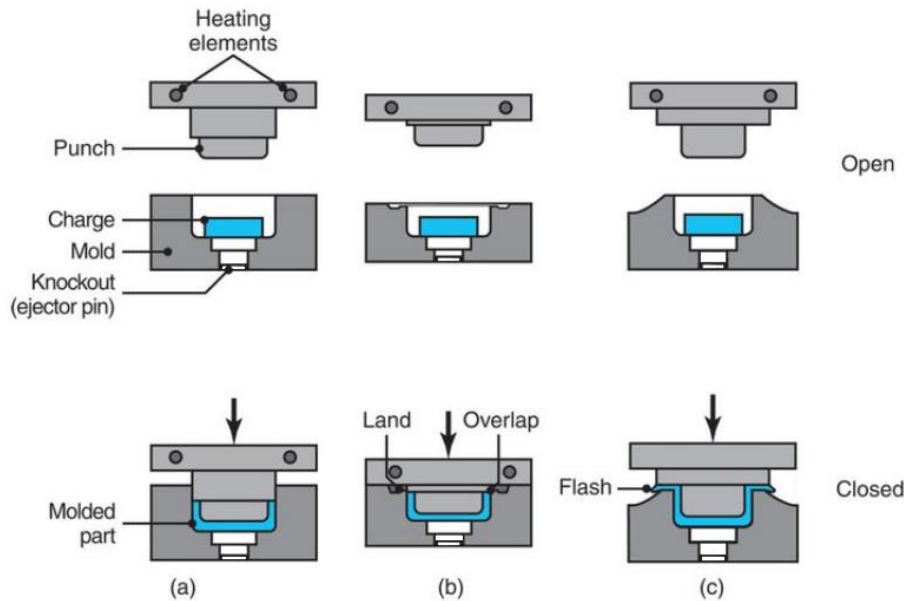


Figure 2.10 - CM Mould Closures Type: (a) Positive; (b) Semipositive; (c) Flash (Adapted from [28])

The first variant, which is called positive type, provides for the introduction of an exact charge to be introduced in the mould in order to allow a complete seal of the two halves of the mould. The quantity of material has to be carefully measured since any excess or deficiency could affect part dimensions. In the event of a severe overcharge it may be impossible to close the two halves of the mould, while a significant deficiency can lead to an incomplete product [26][27].

The semipositive type, by far the most popular, differs from the previous model in the desired presence of an excess of material that creates a very thin layer of attached flash, which will require little postprocessing. This closure ensures a high degree of compaction, leading to excellent properties [26][27].

The last mould closure type, called the flash type, is the simplest and least expensive of the three types. It is characterized by a slightly overcharged cavity so as to allow the excess

material to escape from the main cavity and end up in a flash cavity, specially built for it, leaving a fully formed part. Clearly also this type of closure has to receive a postprocessing operation, in order to trim off the flash cavity and flash ridge, that is the channel between the product cavity and the flash cavity. The products obtained with this solution manage to achieve only a medium part definition, together with the possibility of obtaining an inconsistent density and therefore mediocre physical and mechanical properties [26][27].

The whole machine, given its weight, is usually positioned on its own support structure, or possibly on a sturdy table or on a platform [26].

2.3.1 Process Description

The CM process is one of the simplest among the plastic processing methods and its moulding cycle generally takes from a few minutes to an hour, depending mainly on the type of plastic used and the size of the final product.

The process begins with the preparation of the charge, which is first weighted and usually preheated. The material is then charged into the lower half of the mould, which has previously been heated to the chosen temperature by the heaters placed in the platen or in the mould itself. Once this is done, the press can be closed to melt the material and completely fill the cavity between the two halves of the mould. The plastic is then kept in the mould under the required temperature and pressure for a fixed time [25][26][27].

At this point the process takes different paths according to the type of material: in the case of a thermoset, the plastic continues to be kept in the mould in the same condition to ensure a proper cure, and then undergo a possible cooling phase in the event of large moulds. In the case of a thermoplastic, on the other hand, it is only necessary to cool the material, once again under pressure, to solidify it and avoid any deformation after ejection [26][27].

Now the part is ready to be removed from the mould cavity, the pressure is released and the mould is opened, allowing operation of the ejection system which ejects the final part. The machine is then ready to start another cycle [26][27].

2.3.2 Process Parameters

The CM process, being relatively simple, has few main parameters capable of managing the whole process. The parameters which are examined below are: quantity of moulding material, mould temperature, ejection temperature, mould pressure, compression time and overall cycle time.

The amount of moulding material represents the amount of polymer that will be charged in the lower part of the mould. A correct choice is particularly important if the machine adopts a positive mould closure, due to the problems that could occur in the event of a severe overcharging or a significant deficiency, i.e. preventing the complete closure of the mould or obtaining an incomplete product. In addition to the size of the mould cavity, the choice of the quantity has to consider the flash that will be produced as well as the shrinkage of the material [26].

The mould temperature is the temperature that the heaters have to guarantee for a proper melting and curing. Sometimes the heaters, as well as the temperature sensors, are positioned in the platens, therefore the real temperature in the mould can be different due to the limited thermal capacity of the tool material. A higher mould temperature reduces the mould pressure required, it accelerates the curing phase and it reduces the final warpage, but it requires an additional cooling time. Furthermore, if the heat is too low or too high, filling of the cavity may be difficult, even by increasing the pressure [25][26].

The ejection temperature depends on the type of polymer: in the case of a thermoplastic it is necessary to cool the part until it reaches a temperature for which the deformation is reduced to the minimum possible value. On the contrary, using thermosets, if the mould is small it is possible to directly eject the part immediately after the end of the compression stage, while in the case of larger and more complex moulds it is necessary to wait for the end of the cooling stage. In any case, the ejection temperature strongly depends on the single material used [25][26].

The mould pressure is the maximum pressure ensured by the hydraulic system to melt and make the material flow throughout the cavity, to then ensure, together with the temperature, an adequate curing/cooling phase. The ideal pressure value is obtained when the lowest

viscosity occurs, ensuring a relatively stress-free part and good surface quality. Better results can also be obtained by using a variable-pressure loading, which improves the melt flow during curing [25][26][27].

The compression time, one of the most important parameters involved in the process, at the same level as the mould temperature and the mould pressure, is the time in which the CM machine has to simultaneously apply the mould pressure and the mould temperature to the material in the mould, in the case of a thermosetting material, in order to perform a complete curing. When instead using a thermoplastic, the compression time has the task of cooling the part, once again under pressure but with decreasing temperature. In general, leaving the material at high pressure and high temperature for an excessive time may lead to degradation of the material, but a slight increase in the compression time will accelerate the curing and reduce warpage [25][26][27].

The overall cycle time is constituted by the total time taken by the process to produce a complete part, or a set of parts in the case of a multicavity mould, and it is generally composed of the times used for loading, mould closing, degassing, compression, mould opening and part ejection. Of these operations, the most time consuming is the compression time, because it has to provide proper curing or sufficient cooling to the part. Minimize the cycle time allows the process to be used effectively in the industrial sector, and some solutions to this may be the use of preforms, preheating, in this case mainly because it is done externally, or by introducing automation [25][26][27].

2.4 Composite materials for SLS, IM and CM

A composite material consists of two or more separate materials, with chemically and physically different phases separated by a distinct interface, which are combined into a structural unit. They are made from different combination of metals, polymers and ceramics, where polymers are undoubtedly the most widely used matrix materials nowadays [29][30].

Given this net division, it is possible to differentiate a matrix phase, called also continuous phase, and a reinforcement phase, which is surrounded by the previous phase. The synergetic effect of these two phases aims to improve the properties that the individual components do

Chapter 2. State of the Art

not have. In fact, the main tasks of the matrix are to hold the fillers, protect them, transfer and distribute the applied load, while the reinforcements have to improve the selected properties of the composite [30][31].

Referring to the technologies used in this work, the most used composite materials are polymer matrix composites (PMCs), that is to say a type of composite consisting of particles or fiber embedded in a polymer matrix. These composites are generally divided into three categories based on the type of polymer that is used as a matrix: thermoplastic matrix composites, thermosetting matrix composites and elastomeric matrix composites. The three types of polymer will in fact influence the processing technique used, the cost, the type of reinforcement element and the end use [31][32].

Instead, reinforcements in PMCs can be classified, according to the nature of the material, into four categories: metallic fillers, ceramic/glass fillers, carbon-based fillers and organic additives. Among them, the ceramic/glass fillers are certainly the most used, above all thanks to the composites reinforced with glass fiber which represents the largest class of PMCs. This first type of composite materials highlights another possible classification, namely that based on the type of reinforcement: particulates composites, fiber-reinforced composites, laminate composites and film composites. The most common category is fiber-reinforced composites, where another very important composite is the carbon fiber reinforced PMC, due to his predominant role in the structural area [29][30][31][33][34].

As for the use of PMCs in SLS, the first thing that can be noted is the extensive use, once again, of polyamides as matrix: PAs or PA-based thermoplastic composites occupy up to 95% of the market of powder-bed fusion processes, therefore also SLS. The reason for this predominance lies in the ability of these polymers to meet the stringent requirements of this type of process [4][35].

As far as the reinforcement materials are concerned, a wide spectrum of reinforcements has been used in SLS. In most cases, the reinforcement powder is used as particulate because fibers give problems in the process, especially as regard the powder bed formation. This problem has been solved in recent years thanks to the transition to the use of nanomaterials [4][36][37].

One of the most used reinforcement in SLS is represented by glass beads, followed by CNTs, carbon nanofibers (CNFs), nanoclays, nanosilica and many others [4][35]. Some examples of composite material for SLS are shown in the following Table 2.1

Table 2.1 - Example of PMCs in SLS

| Polymer Matrix | Reinforcement | References |
|-----------------------|----------------------------|---------------------|
| PA12 | Glass Bead | [35, 37] |
| | Cu | [35] |
| | Al | [35, 37] |
| | SiC | [35, 36] |
| | GNP | [4, 38] |
| | Nanosilica | [4, 38] |
| | CNT | [4, 36, 38, 39, 40] |
| | Carbon Black | [4, 38, 40] |
| | CF | [39, 40] |
| | Nanoclay | [36, 40, 41] |
| | CNF | [36, 40, 41, 42] |
| PA11 | GNP | [4, 36, 40] |
| | CNT | [4, 40] |
| | Nanoclay | [4, 36, 41, 43] |
| | CNF | [4, 36, 41, 43] |
| | Glass Bead | [37, 38] |
| | Nanosilica | [38, 41] |
| PA6 | Yttria-stabilized Zirconia | [36] |

Chapter 2. State of the Art

| | | |
|------|-------------------------------------|----------|
| PA6 | Nanoclay | [38] |
| PEEK | CF | [4, 35] |
| | HA | [37] |
| | GP | [44] |
| PVA | Calcium Silicate | [45] |
| | HA | [37] |
| PMMA | HA | [37] |
| | SiC | [46] |
| PEKK | CF | [4] |
| PU | CNT | [4] |
| PCL | Nano HA | [37, 45] |
| PC | Graphite | [36, 37] |
| HDPE | HA | [35, 37] |
| PVC | HA | [35] |
| PLLA | HA | [37] |
| PS | Nano Al ₂ O ₃ | [35, 37] |

As regard instead IM, the spectrum of matrices and reinforcements is in general much wider than that present in SLS. This difference is particularly evident in the choice of the matrix, a possibility given by the ability of IM to process a greater quantity of polymers. The materials most used as matrix are PAs and PP, following by all the polymers most used in traditional IM, such as PE, ABS and polyesters (PET) [18][20][24][31].

Unlike SLS, in IM the fibers of different materials are the most used reinforcements in PMCs, where short glass fibers are by far the most common type. Other examples of reinforcements used are carbon fiber, clay, carbon black, etc. [18][20][24][31].

Some examples of composite material for IM are shown in the following Table 2.2

Table 2.2 - Example of PMCs in IM

| Polymer Matrix | Reinforcement | References |
|-----------------------|----------------------|-------------------|
| PP | Talc | [24, 31] |
| | GF | [20, 24, 31] |
| | Nickel-coated GF | [24] |
| | Nanoclay | [24] |
| PA6 | GF | [20, 24, 31] |
| | Nanoclay | [18, 24] |
| | Carbon Black | [24] |
| | Long GF | [24] |
| PA66 | GF | [18, 20, 24, 31] |
| | Long GF | [24, 31] |
| PA6.12 | GF | [20] |
| HDPE | GF | [24, 31] |
| PE | GF | [20] |
| PET | GF | [20, 24, 31] |
| ABS | GF | [18, 20] |
| PC | GF | [20] |
| PS | GF | [20] |
| PU | GF | [20] |
| PVC | GF | [20] |
| PI | GF | [24, 31] |

Chapter 2. State of the Art

| | | |
|-----------------|----|----------|
| PPE | GF | [20] |
| PPS | GF | [20] |
| Polyimide-imide | GF | [24, 31] |
| PBT | GF | [24, 31] |
| PSU | GF | [20, 31] |
| SAN | GF | [24] |

Finally, as far as CM is concerned, this technology differs from the previous two for the extended use of the so-called ‘premix’, that is a moulding compound usually consisting of reinforcing fibers, fillers and polymer as a matrix. An important feature of a premix is that it does not require any further processing after its manufacture and that it is therefore ready to be used in the moulding press. There are many forms of premix used in CM, but the most important are Sheet Moulding Compound (SMC), Dough Moulding Compound (DMC) and the Glass Mat Reinforced Thermoplastics (GMT). Globally, the compression moulding of SMC represents about 15% of the total parts produced with composite materials, ranking third in the most used techniques for the production of polymer composite parts [26][31][47][48].

SMC has been the most used form of material used for CM since its introduction in the early 1970s. A typical SMC consists mainly of fibers (usually E-glass fiber), a thermosetting polymer (usually based on unsaturated polyesters) and fillers (usually calcium carbonate). Fibers are also usually used as bundles and various other types of fibrous reinforcement can be used, such as carbon fibers, plant-based fibers or hybrids. As regard the thermosetting materials, other solutions mainly concern phenolic resins, vinyl ester resins, epoxy resins and bio-based resins. The fillers used are mainly minerals and some examples are clay, talc, alumina, carbon blacks, etc. Recent attention has been captured by some possible substitutions for the filler, usually calcium carbonate, to reduce the total weight of the SMC composites, introducing glass beads, nanocomposite fillers and carbon fibers [26][31][48].

DMC, also called Bulk Moulding Compound (BMC), has a composition very similar to SMC as it is also composed mainly of fibers, thermosets and fillers. E-glass fibers still remain the most used material as fibers, but others are used such as carbon, aramid, wood, sisal, asbestos and chopped nylon rag. The differences between this type of composite and the previous one lie in the final form, this time produced with a dough-like form, the lower fiber content and their shorter length. The consequences are fewer mechanical properties than SMC [26][31].

Regarding the last type of premix analysed here, the main difference between GMT and the previous two is the use of a thermoplastic instead of a thermosetting one. The main components of a GMT sheet are in fact a thermoplastic as matrix and a reinforcing fiber, where the most popular matrix material is polypropylene, followed by other thermoplastics such as polyamides, polycarbonate and PVC. The most common reinforcing fibers are also in this case E-glass fibers[31].

Recently, GMTs, together with a variant called Long Fiber Reinforced Thermoplastics (LFRT or LFT), have been widely used in the CM process, in particular as structural components in the automotive industry [26][31].

2.4.1 Graphite-based composites

Graphite is one of the material used as filler in the field of PMCs where, in most cases, it is mainly used for its ability to greatly improve the electrical properties of the matrix with which it is added, which are normally almost zero given the insulating nature of polymers. The addition of graphite is also used to improve thermal conductivity, flame retardancy, mechanical properties, friction-reducing, anti-wear behaviour and, in the specific case of SLS, the reduction of the laser energy necessary to sinter the polymer chosen as matrix. The increase in these properties is due to the greater electrical, thermal and mechanical properties of graphite compared to those of polymers [20][26][30][31][32][33][34][45][47][48][49].

In relation to the use of graphite powder in PMCs, the most used matrices are mainly epoxy resin, polyethylene and polyamides. Some examples of PMCs with graphite as filler are shown in Table 2.3.

Chapter 2. State of the Art*Table 2.3 - Example of Graphite as Filler in PMCs*

| Polymer Matrix | Reinforcement | References |
|-----------------------|----------------------|-------------------|
| Epoxy | Graphite Powder | [48, 50, 51] |
| HDPE | Graphite Powder | [52, 53, 54, 55] |
| LDPE | Graphite Powder | [55, 56] |
| PA6 | Graphite Powder | [52, 57, 58] |
| PA12 | Graphite Powder | [59] |
| ABS | Graphite Powder | [48, 52] |
| PP | Graphite Powder | [52, 60] |
| PS | Graphite Powder | [52] |
| PMMA | Graphite Powder | [52] |
| PC | Graphite Powder | [49] |
| NBR | Graphite Powder | [52, 61] |
| SBR | Graphite Powder | [62] |
| Vinyl Ester | Graphite Powder | [31] |
| HIPS | Graphite Powder | [52] |
| PTFE | Graphite Powder | [26] |
| Basalt fabric | Graphite Powder | [48] |
| PI | Graphite Powder | [48] |
| EVA | Graphite Powder | [52] |
| SR | Graphite Powder | [52] |
| PEN | Graphite Powder | [52] |
| POM | Graphite Powder | [52] |
| PVDF | Graphite Powder | [63] |
| Polyphenylene | Graphite Powder | [64] |

| | | |
|-------------------------------|-----------------|------|
| PDMS | Graphite Powder | [65] |
| Epoxy (+ CF) | Graphite Powder | [51] |
| Epoxy (+ GF) | Graphite Powder | [66] |
| TPV/PP-g-MA | Graphite Powder | [52] |
| PI (+ CF + SiO ₂) | Graphite Powder | [67] |

2.4.2 Carbon Nanotubes-based composites

Carbon Nanotubes (CNTs) are rolled-up structures of individual sheets of graphene that form cage-like hollow tubes with a diameter of several nanometers. Two types of nanotubes are mainly used: the single walled carbon nanotube (SWCNT) and the multiwalled carbon nanotube (MWCNT). The difference lies in the different number of graphene cylinders from which they are composed, i.e. only one in the case of a SWCNT while a MWCNT can be described as several coaxial cylinders connected together by weak van der Waals forces [31][47][48].

In recent years, CNTs are one of the reinforcement material that have received the most attention in the PMCs area, leading the recent revolution of nanotechnology, mainly thanks to their outstanding structural, mechanical, electrical and thermal properties. Inserted in what is called a nanocomposite due to the nanoscopic size of the filler, CNTs have proven to be able to significantly improve the mechanical, thermal and above all electrical properties of the pure matrix polymer. Other important properties can be improved with this kind of filler such as flame retardancy, internal damping, creep resistance, smooth surface finish and lower part warpage [29][30][31][33][38][47][48][68].

As regards the electrical properties, using CNTs the achievement of the percolation threshold was observed, i.e. the critical filler concentration above which the conductivity of composite increases dramatically, with a much lower load than the larger traditional fillers, due to the low size, high aspect ratio, high surface area and low density of the CNTs. [2][48][69].

In the field of PMCs, CNTs have been introduced into the most used polymers, as well as particular polymers as conductive polymers, e.g. polyaniline (PANI), polypyrrole (PPy),

Chapter 2. State of the Art

Poly(3,4-ethylenedioxythiophene) (PEDOT). Some examples of PMCs with CNTs as filler are shown in Table 2.4.

Table 2.4 - Example of CNTs as Filler in PMCs

| Polymer Matrix | Reinforcement | References |
|-----------------------|----------------------|------------------------------|
| ABS | CNT | [68] |
| Epoxy Resin | CNT | [29, 38, 45, 68, 69, 70, 71] |
| HDPE | CNT | [31, 48] |
| LDPE | CNT | [48] |
| HA | CNT | [47, 68] |
| PA11 | CNT | [33, 40] |
| PA12 | CNT | [33, 38, 39, 68] |
| PA6 | CNT | [69, 70] |
| PAN | CNT | [71] |
| PANI | CNT | [47, 48] |
| PC | CNT | [29, 48, 68, 70] |
| PCL | CNT | [48] |
| PDMS | CNT | [48, 70] |
| PE | CNT | [48, 68, 69, 70] |
| PEDOT | CNT | [47, 48] |
| PEEK | CNT | [38, 70] |
| PEG | CNT | [31, 48, 68] |
| PET | CNT | [48] |
| Phenolic Resin | CNT | [47] |
| PLA | CNT | [45] |

Chapter 2. State of the Art

| | | |
|------|-----|--------------------------|
| PMMA | CNT | [29, 47, 48, 68, 69, 70] |
| PP | CNT | [48, 68, 69, 70, 71] |
| PPy | CNT | [47, 48] |
| PS | CNT | [31, 48, 68, 69, 70, 71] |
| PSU | CNT | [38] |
| PU | CNT | [47, 68, 70] |
| PVA | CNT | [31, 48, 68, 69, 70, 71] |
| PVC | CNT | [68] |
| PVDF | CNT | [47, 70] |

Chapter 2. State of the Art

Chapter 3. Experimental component

This chapter provides a complete detailed description of the experimental component conducted in this research. In particular, it contains the experimental methods used, equipment, material, methodology, principles and the conditions of the processes, as well as the characterization tests with which the final parts were analysed.

3.1 Methodology description

The experimental approach of this work involved the production of a sufficient number of test specimens using various PA12-based mixtures both through SLS, IM and CM, and then subjecting the specimens to characterization tests in order to understand how the processes affect the final properties of the parts. The materials used in this work were an unfilled PA12 (trade name PA220 from EOS GmbH), graphite (waste from an industrial electrical discharge machining process) and carbon nanotubes (multiwalled carbon nanotubes).

The machines used were a BOY22A for injection moulding, a Sinterstation 2500 for SLS and a CM equipment supplied by M. J. AMARAL *Lda*.

The comparison between the three different technologies of SLS, IM and CM was performed trying to replicate the same conditions as much as possible, even if some choices were not optimal for one of the three processes. One of the most important choices concerned the use of powdered material in the IM process instead of granules, which would probably guarantee better performances, because they could not be used in SLS.

3.2 Composite preparation

The starting point of the three processes lied in the process of mixing the material involved. The method chosen to obtain the desired mixture was a mechanical mixing, in which the correct percentages of PA12 and filler were poured into a bag, the bag was closed and then the materials inside were agitated for a few minutes. The reason behind this method's choice lies in the ease of this solution combined with the possibility of applying it to all the processes considered. Although this technique is not the best in terms of results, it is the most used in SLS. It should be noted that other methods would probably give better results and they should be considered for future works [5].

The final used mixtures were: i) unfilled PA12; ii) PA12 with 1/3/5/10/30% graphite by weight; iii) PA12 with 3% CNT by weight; iv) PA12 with 10% graphite and 1.5/3% CNT by weight. The mixtures were prepared immediately before the start of the processes in order to guarantee less contamination with the environment.

As far as PA12 is concerned, a dehumidification phase was necessary to reduce the humidity inside the material to the right amount, since polyamides are hygroscopic materials, and this could cause some problems during the processes. This operation was performed by using a dehumidification machine (BINDER heating chamber with forced convection) in which the material has to remain for 2 hours at 80 °C, since the PA12 was not totally virgin because a part of this was previously subjected to the SLS process, making it necessary to have a lower temperature. After this time the material could be used and, in order to maintain proper storage of the unused material, the temperature inside the dehumidification system was lowered to 40 °C [3].

As for the total quantity of powder mixture prepared for each process, it differs according to the technology. The machine used for the SLS needed around 3 kg for each mixture to produce the 10 desired specimens, due to the need to completely fill the two reservoirs. IM and CM machines needed a small amount of powder, around 0,3 kg to produce the same number of specimens for each condition.

3.3 Composite processing by Selective Laser Sintering

The first step to produce parts through the SLS technology is the creation of the CAD model of the desired product. The selected part geometry for this work is the type 5A, defined by ISO 527 [74]. The specimen was modelled using the software AutoCAD and the result is shown, with the dimensions in millimetres, in Figure 3.1.

Chapter 3. Experimental component

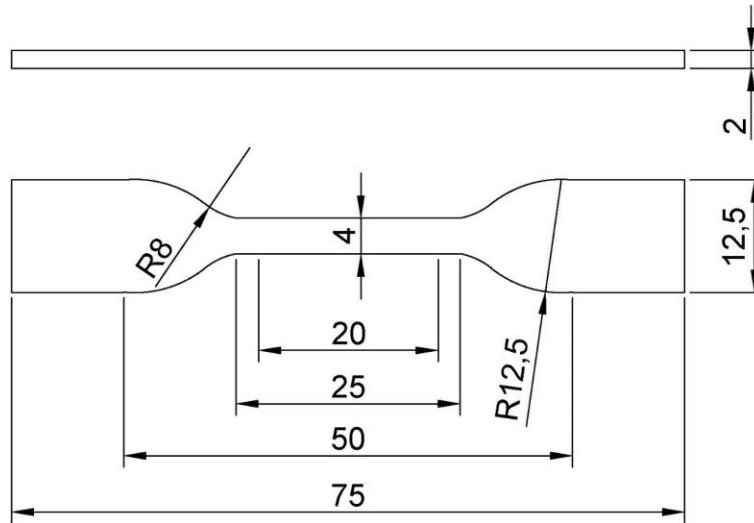


Figure 3.1 - SLS Dogbone Specimen Dimensions

The model was then transformed in a 3D file through an STL format and transferred to the main computer of the Sinterstation 2500. Providing a good model of the object is essential to obtain a good quality of the part and a correct building process [3].

The file was opened in the software where it was possible to set the chosen parameters for the process, which were chosen using the datasheet and the standard relating to PA12.

After checking all the parameters involved, the process can be started. After the end of the process, including the necessary cooling phase, the specimens can be removed from the powder bed and they can be cleaned using a compressed air system, removing as much unused powder as possible.

As regards the mixtures used, the idea behind the choice was the same as that for IM, that is to go to produce and analyse only the mixtures that presented the best properties. This idea clashed though with the real possibility to introduce high amount of CNT inside a polymeric material that was already highlighted by other authors [33][75][76].

3.4 Composite processing by Injection Moulding

The injection moulding process begins with the assembly of the mould inside the main injection moulding machine. This operation requires a lot of attention as the mould is heavy and it can cause a lot of damages in the surrounding areas.

The chosen mould had two cavities with the non-standard dog bone shape. The nominal dimensions of the samples are shown in Figure 3.2.

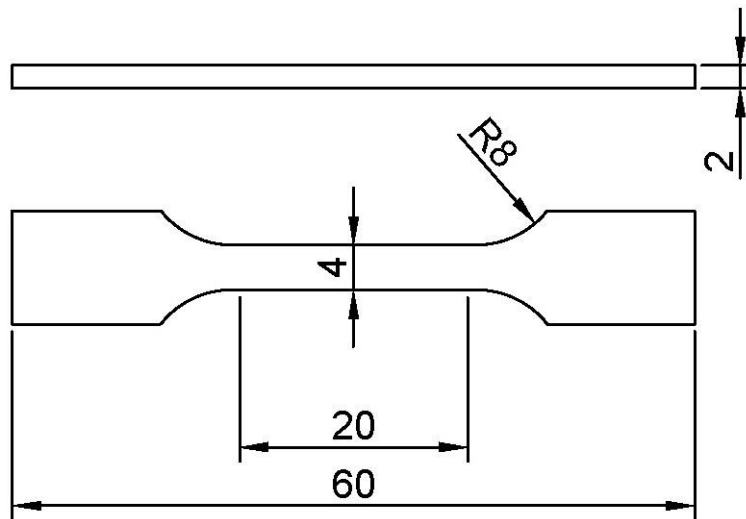


Figure 3.2 - IM Dogbone Specimen Dimensions

After assembling the whole mould, a calibration phase of both the mould and the ejection system was necessary, in order to ensure correct initial positioning of the two halves of the mould and a correct stroke of the ejectors. It is important to check that all the movements inside the machine are free and that they do not cause damage to the machine during the process.

At this point, the process has to be optimized to produce the best possible result. The optimization mainly concerned the temperature along the barrel, the pressures, the hold time and the injection speed. As a starting point it is possible to use the values of the datasheet provided by the manufacturer and therefore the best method consists in the physical observation of the products obtained, followed by some adjustment to solve the problems or improve the quality of the outcomes.

Chapter 3. Experimental component

In this work, the optimization was carried out for pure PA12 and therefore the parameters obtained were kept the same for all the mixtures, in order to compare them without the influence of the process parameters. The most important parameters are shown in Table 3.1.

Table 3.1 - IM Process Parameters

| Parameter | Value | | | | |
|---------------------------------|--------------|-----|-----|-----|-----|
| Temperature Profile [°C] | 250 | 240 | 220 | 200 | 180 |
| Mould Temperature [°C] | 50 | | | | |
| Injection Pressure [bar] | 80 | | | | |
| Hold Pressure [bar] | 20 | | | | 10 |
| Back Pressure [bar] | 60 | | | | |
| Overall Cycle Time [s] | 29 | | | | |
| Injection Time [s] | 0,56 | | | | |
| Cooling Time [s] | 20 | | | | |
| Hold Time [s] | 3,5 | | | | |
| Injection Speed [mm/s] | 60 | | | | 50 |
| Screw Speed [rpm] | 500 | | | | |
| Shot Size [mm] | 26 | | | | |

After the optimization, the process can operate in automatic mode, necessary to guarantee the repetitiveness of the process itself. In this condition the specimens for the characterization tests were manufactured, checking the weight of consecutive specimens to avoid fluctuations of the parameters in the process. After waiting for a limited number of cycles, it is possible to collect the ten specimens needed for the tests. To obtain two dogbone specimens it was necessary to cut the products of the IM process and this further operation was completed using a cutter.

At the end of the process, the machine has to be cleaned, focusing on the screw to completely remove the material inside, especially if fillers have been used.

As regards the mixtures used, the research began by taking into consideration the literature on the results obtained with the introduction of graphite as reinforcement in the polymeric materials produced by IM, CM and SLS, focusing on the percentage necessary to reach the percolation threshold. Following the percentages used in those papers, the mixtures initially chosen were unfilled Polyamide 12, Polyamide 12 with 1%, 3% and 5% by weight of graphite [49][57][63][72][73].

After finding unsatisfactory properties, especially with regard to electrical and thermal properties, the chosen percentage of graphite was further increased to 30%, in order to find the percolation threshold with that process. In addition to this increase in graphite, multiwalled carbon nanotubes were chosen as a possible additional reinforcement capable of improving the properties sought. Two other mixtures were therefore studied: PA12 with 30% graphite by weight; PA12 with 10% graphite and 3% CNT, both by weight. They were also chosen to understand their mutual influence in the processes, with obviously greater attention to the SLS process, the one less studied from the point of view of the reinforcements.

3.5 Composite processing by Compression Moulding

The compression moulding process begins with the choice of the mould shape. In this work a cavity consisting of a thin plate was chosen to obtain, to then obtain dogbone samples through a cutter used in the same machine. The dimensions of the cavity were 200x50x2 mm.

The CM process is easier than the SLS and IM processes, as it does not require any machine calibration phase. The product optimization was obtained through the physical observation of the result, following the literature and the advice of the technicians. The parameters chosen for the best results are shown in Table 3.2 and in Figure 3.3.

Chapter 3. Experimental component

Table 3.2 - CM Process Parameters

| Parameter | Value |
|---------------------------|-------|
| Mould Temperature [°C] | 200 |
| Mould Pressure [bar] | 100 |
| Ejection Temperature [°C] | 50 |
| Melt Time [s] | 360 |
| Compression Time [s] | 60 |

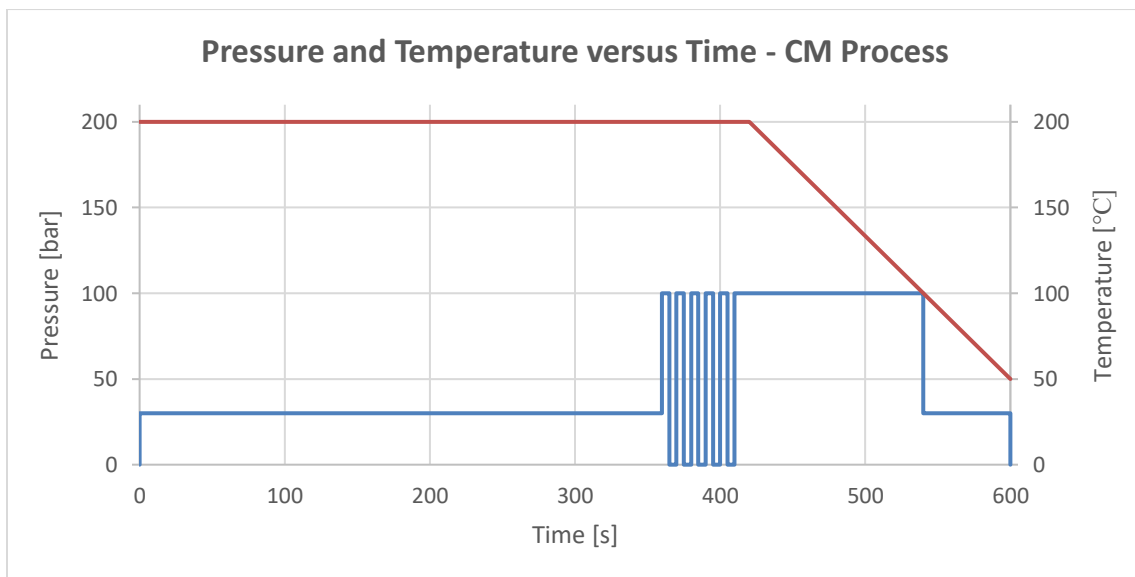


Figure 3.3 - Mould Pressure and Mould Temperature versus Time in CM Process

In the Figure 3.3 it is possible to see the trend of mould pressure and mould temperature during the process. The initial melting phase, characterized by the maximum temperature of the mould and low pressure, is followed by a compression phase, with the maximum mould temperature and mould pressure. This phase is characterized by a continuous up and down movement of the lower mobile base, which proceeds to apply maximum and zero pressure to the material intermittently. In this case it is represented by an idealization since it is difficult to define the real time used. Finally, a cooling phase initially cools the material under the

maximum pressure and decreasing temperature, and then continues, after reaching 100°C, at minimum pressure, until the ejection temperature is reached.

After the production of the plates, a cutting phase was necessary to obtain the correct shape of the samples. This important operation was carried out using a cutter, again using the compression moulding machine. The geometry of the part selected for this job is the same as SLS process, that is the type 5A defined by ISO 527 [74]. The dimensions of the CM samples are shown in Figure 3.4.

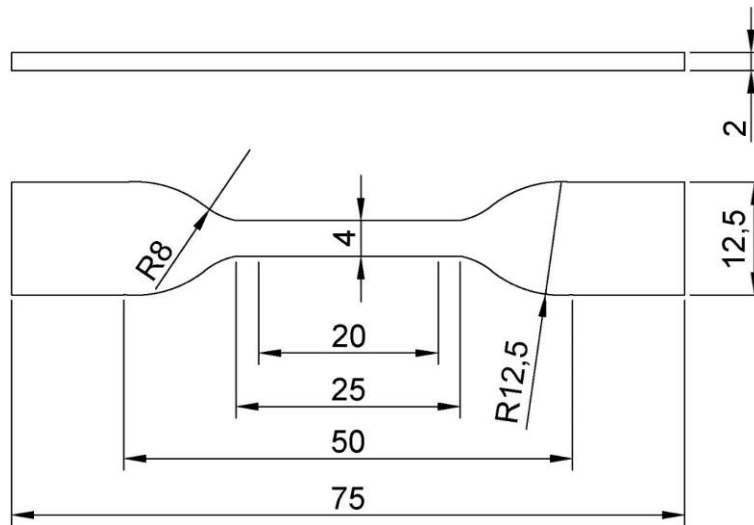


Figure 3.4 - CM Dogbone Specimen Dimensions

After production, a cleaning phase may be necessary due to the cutting operation.

At the end of the process, the machine has to be cleaned, focusing on the Teflon sheets and the mould, in particular on the latter which is the most difficult part to clean and can require a lot of effort.

As for the mixtures used, they were chosen based on the results obtained from the IM samples, going to produce and analyse only the best solutions. Based on this idea, the mixtures used were the following four: unfilled PA12, PA12 with 30% graphite by weight, PA12 with 3% CNT by weight and PA12 with 10% graphite and 3% CNT by weight.

3.6 Characterization tests

The specimens obtained from the different mixtures and from the different technologies were then assessed through dimensional, mechanical, electrical, thermal and microstructural tests to characterize the properties of each solution. The characterization tests and their experimental conditions are summarized in Table 3.4.

Table 3.3 - Characterization Tests

| Test | Description and Experimental Conditions |
|--|--|
| Evaluation of Mass and Dimensions Variation | A Kern PCB Balance is used to determine the mass and a Garant DC2 Calliper to determine the height, the width and the thickness, in order to evaluate the dimensional accuracy of the samples. All the samples were subjected to this test. |
| Tensile Test | An Instron 5969 Universal Testing System with video extensometer and a 50 kN load cell was used to measure the mechanical properties of materials, such as Young's Modulus, Yield Strength, Fracture Strength, Fracture Strain and Ultimate Tensile Strength (UTS). Six samples were studied for each condition, at 10 mm/min. |
| Differential Scanning Calorimetry (DSC) | A Netzsch DSC 200 F3 Maia was used to perform the DSC analysis to analyse the thermal properties, such as Thermal Resistance and Thermal Conductivity. A Perkin Elmer AD-4 Autobalance was used to evaluate masses. The samples were studied at a flow rate of 10 °C/min starting from 20 °C to 180 °C in a constantly purged nitrogen atmosphere. |
| Electrical Test | An electrometer was used to measure the electrical properties of materials, such as Electrical Resistance and Electrical Conductivity. Three samples were used, and they were studied under a 10 V voltage. |
| Microstructural Test | A Ultramicrotome Leica EM UC6, with glass knives, was used to prepare ultrathin sections of 2 µm from the cross section of the specimens. Subsequently, a Transmission Olympus Microscope (Brighfield microscopy) was used to capture the pictures of the cross |

| | |
|---|---|
| | sections using 2x, 4x, 10x and 20x magnification for each specimens. |
| Scanning Electron Microscope | A Scanning Electron Microscope (SEM) was used to capture the pictures of the cross sections using 130x, 500x, 1000x, 5000x, 15000x, 50000x and 100000x magnification for a selected specimen set. |

Between production and sample tests, the samples were stored in a room with a controlled environment at 22 °C and 40% RH. All tests were conducted at room temperature.

Chapter 3. Experimental component

Chapter 4. Discussion of the Results

This chapter critically examines the results from the characterization test performed on the different mixtures specimens. The results are interpreted taking into account the previous state of the art, comparing the different technologies, the different fillers and their mixing ratios.

4.1 General Consideration about the Manufacturing Processes

Although most of the test samples were of good quality, some problems affected the work during the manufacture of the specimens, sometimes generating non-compliant samples or the need to change some parameters. The following are the most common difficulties that occurred during the experiments.

As for Injection Moulding, the parameters chosen by the process optimization for pure PA12 caused problems when they were then applied to composites. The main problem arose with the increase in the amount of filler inside the polymer, with a consequent increase in the part sticking problem. Using the composite composed of PA12 with 5% graphite, the problem made it necessary to use a manual ejection, and therefore it did not allow the use of the automatic mode, generating a slight bending in the direction of ejection.

Regarding PA12, due to the choice to start with composite materials and to end with pure PA12, the test specimens showed a small presence of black points due to the fillers remaining inside the screw, a known problem when polymers with fillers are processed (Figure 4.1). The presence of those fillers was reputed irrelevant to the results of the characterization tests.



Figure 4.1 - PA12 Sample with Black Point Produced by IM

As for Compression Moulding, the first main problem arose from the very manual nature of the process used, which involved a few trial and error processes to find the minimum quantity of material, while remaining one of the most significant unknowns. Due to this problem, the final thickness and density of the manufactured plates could also obtain very different and non-uniform values, leading to the non-repeatability of the process.

Another problem appeared immediately after the opening of the two main moulds, i.e. the bending of both the plate and the die due to the attempt to shrink the former, which collided with the stiffness of the latter. This could lead to a permanent deformation of the die and it also make the extraction of the plate more difficult. After extraction, the plate still maintained a certain deflection that was then partially recovered from the subsequent cutting operation. This problem has been found above all using the mixtures with 10% graphite and 3% CNT.

The sticking of the material on the die is a difficulty encountered when using all types of material, in particular with pure PA12. The cleaning operation on the die took several minutes to ensure proper cleaning of each individual piece of material (Figure 4.2).



Figure 4.2 - CM Die After Process

Finally, in the final cutting operation, the last problem concerned the specimens, which were stuck in the cutter after cutting. This problem was mainly encountered when using composites with 30% graphite, and it required a meticulous operation to remove the specimen without breaking it, also given the brittle nature of the specimen.

The only difficulty during the tensile tests was related to the video extensometer, which sometimes found it difficult to find the points drawn on the specimens. This problem was particularly evident when using grey specimens, probably due to the low contrast between the colour of the points and the specimens.

Chapter 4. Discussion of the Results

As for the thermal tests, the main problem was the interaction between indium and the tested material. To ensure a reliable result from the test, it is necessary to ensure that you have the most complete contact of the indium on the material, but without the indium touching the bottom of the test vessel. This was the most critical aspect of the whole test, which involved repeating some specimens.

4.2 Mechanical Properties

As regards the tensile test, the mechanical properties chosen to describe the behaviour of the specimens subjected to a load were: i) Young's Modulus, ii) Yield Strength, iii) Fracture Strength, iv) Ultimate Strength and v) Elongation at Break.

Given the mechanical properties found, it is possible to define the influence of the introduction of the fillers by dividing the technologies into two groups, based on the behaviour they present.

On one side, using IM it is possible to observe that all mechanical properties decrease using small amount of graphite (less than 5%), probably due to the presence of graphite itself which acts as a defect in the polymeric material, leading to a faster start of the first cracks, which will lead to breakage (Figure 4.3). This general reduction of properties with increasing fillers leads to a remarkable loss, especially with regard to fracture strength, with a loss of about 35%, ultimate strength, with a loss of more than 30%, and maximum elongation, which reaches 63% lower values, compared to the values obtained with pure PA12.

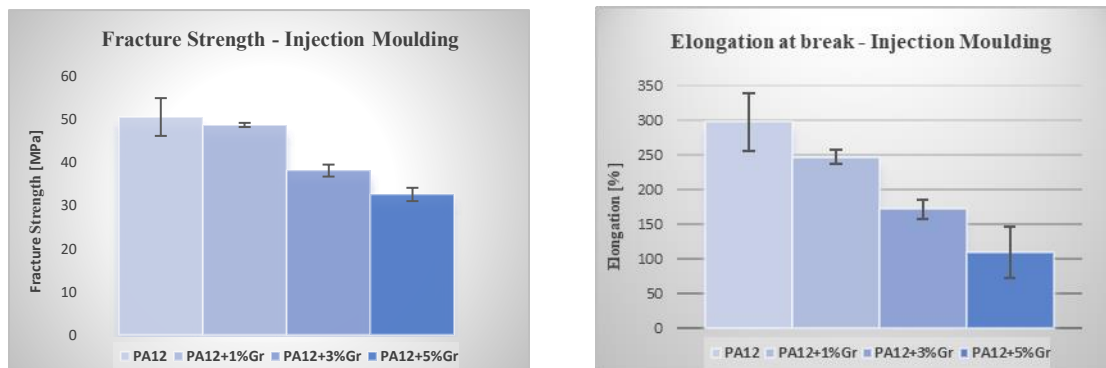


Figure 4.3 - Fracture Strength and Elongation at Break of IM Specimens with Different Amount of Graphite

When it comes to use higher value of graphite, CNT or a combination of these two types of filler, the trend using IM changes (Figure 4.4). The mixture containing 30% of graphite allows to always obtain values equal to or higher than those of the pure polymer, with the exception of the elongation at break that loses almost three orders of magnitude, reaching values 2.5 times higher in the Young's modulus, demonstrating to be able to replace the polymer in many applications where good mechanical characteristics are required, although being very brittle. These results can be attributed to the good dispersion of the mixture, even if it has agglomerates, because they are not so big and well dispersed.

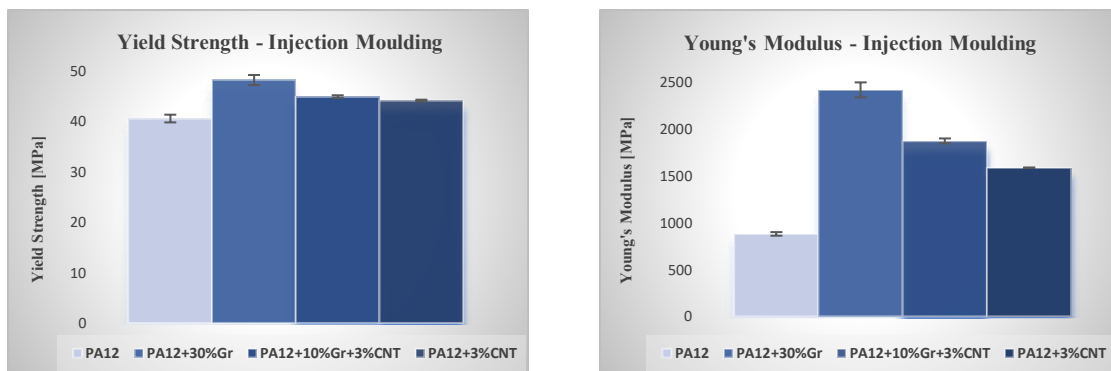


Figure 4.4 - Yield Strength and Young's Modulus of IM Specimens with Different Amount of Graphite and CNTs

Using CNTs and the combination of graphite and CNTs, the resulting mechanical properties revealed an intermediate behaviour with respect to the two cases listed so far, which obtained higher values for the yield strength and especially the Young modulus, reaching values respectively greater than about 180% and 210%, compared to pure PA12, for the mixture with CNTs and with both, but lower values for the other properties, in particular as regard maximum elongation, in which the test recorded lower values respectively than 65% and 90% (Figure 4.5). These results can be attributed to the reinforcing effects of the filler, which are present, however, in a smaller amount than the solution with 30% graphite, although they also have a good dispersion.

Chapter 4. Discussion of the Results

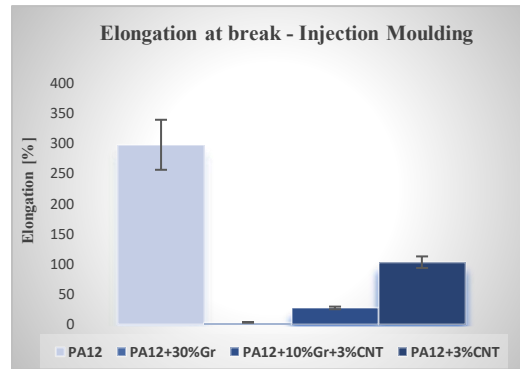


Figure 4.5 - Elongation at Break of IM Specimens with Different Amount of Graphite and CNTs

On the other hand, using CM and SLS the trend of properties is almost always decreasing with the increase in fillers, where the only exception is the Young modulus of PA12 with 30% graphite, which grows by 30% compared to pure PA12 made with CM.

More specifically, within CM the mixture with 30% of graphite achieves the highest or equal values, with the exception of the maximum elongation in which it achieves the lowest, losing 99% of the value of pure PA12 (Figure 4.6). The combination of the two fillers is not advantageous for almost all properties, with the exception of Young modulus and maximum elongation.

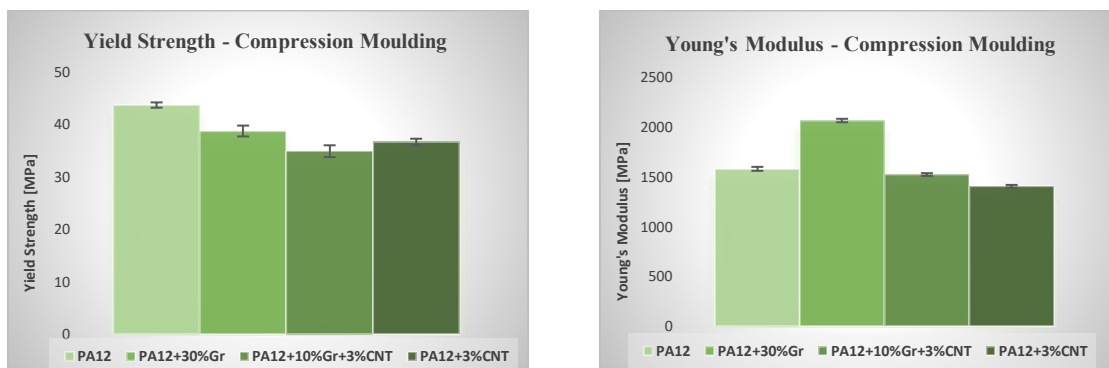


Figure 4.6 - Yield Strength and Young's Modulus of CM Specimens with Different Amount of Graphite and CNTs

As regards SLS, the mechanical properties of the composite with 10% graphite decrease slightly or remain constant, compared to pure PA12 made with SLS, while the addition of CNTs further worsens performance (Figure 4.7).

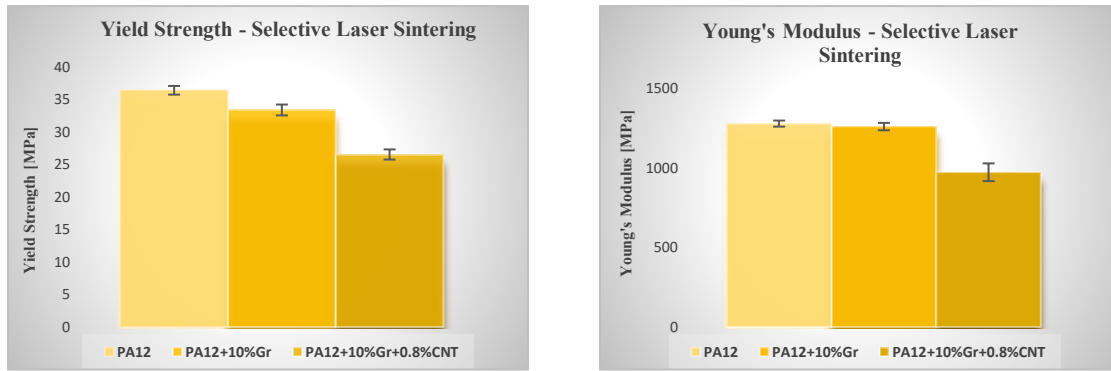


Figure 4.7 - Yield Strength and Young's Modulus of SLS Specimens with Different Amount of Graphite and CNTs

As for the influence of technologies on mechanical properties, a typical trend can be observed in all the analysis (Figure 4.8). The highest values for pure PA12 are always obtained using CM technology, while SLS implies the lowest, with the exception of the Young modulus, in which that of IM reaches the lowest.

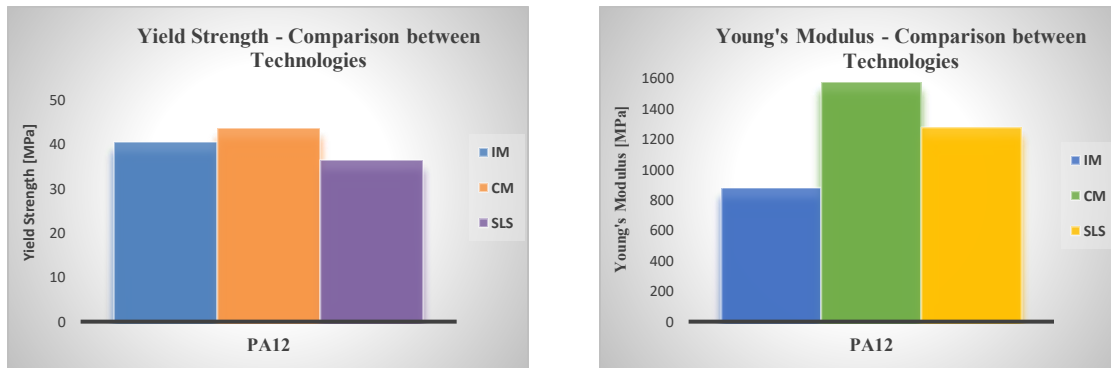


Figure 4.8 - Yield Strength and Young's Modulus of pure PA12 Specimens using IM, CM and SLS

Evaluating composites made up of 30% graphite, 10% graphite plus 3% CNTs and only 3% CNTs, it is clear that in these cases IM allows to always obtain better results than CM, obtained thanks to a better dispersion of the fillers inside the material, observable also through the smaller dimensions of the agglomerates (Figure 4.9).

Chapter 4. Discussion of the Results

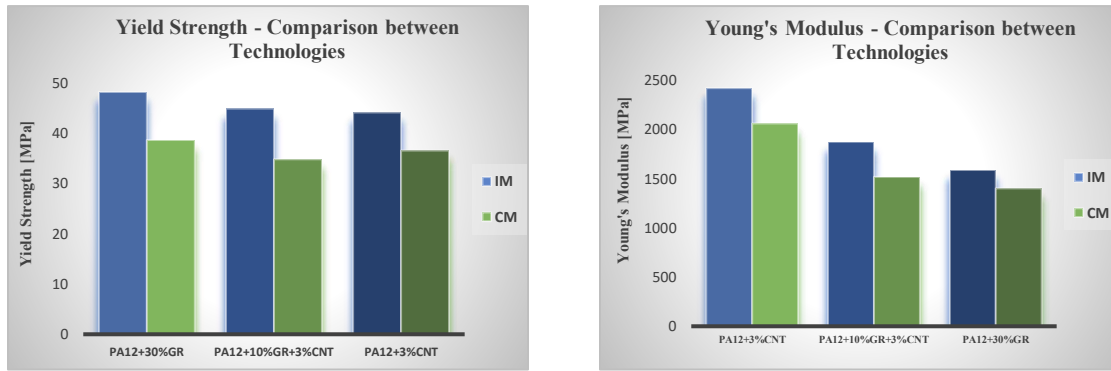


Figure 4.9 - Yield Strength and Young's Modulus of Composite Specimens using IM and CM

Finally, considering at a general level, the solutions that guarantee the best results are mainly two, namely the composite formed by PA12 with 30% of graphite produced by IM and pure PA12 produced by CM. The first guarantees the highest yield strength and Young modulus values, i.e. approximately 48 MPa and 2400 MPa respectively, while the second guarantees the highest fracture strength, ultimate strength and elongation at break, i.e. approximately 54 MPa, 54 MPa and 320% (Figure 4.10, Figure 4.11 and Figure 4.12). Once again it is good to underline that the values of these results are not directly comparable, due to the different quantities of fillers used.

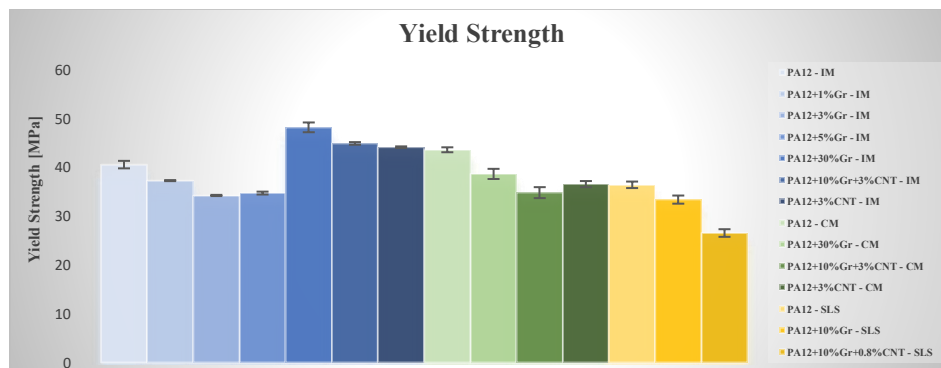


Figure 4.10 - Yield Strength of the Specimens

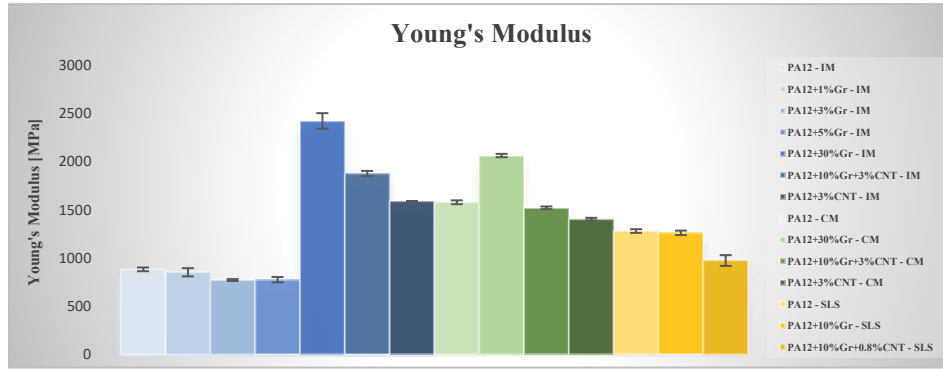


Figure 4.11 - Young's Modulus of the Specimens

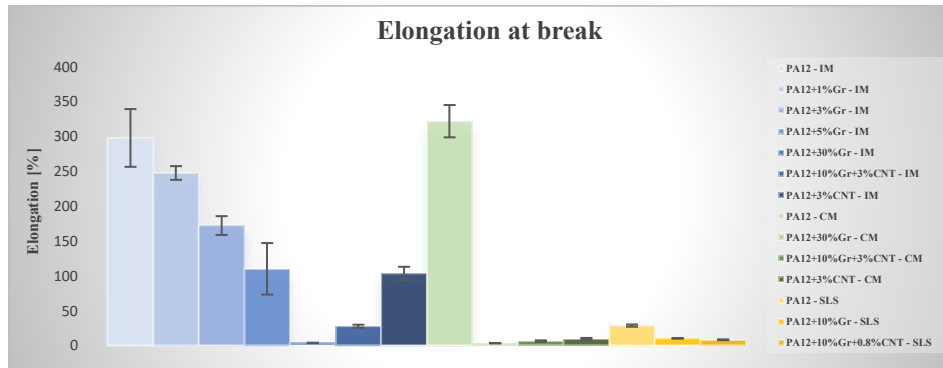


Figure 4.12 - Elongation at break of the Specimens

4.3 Electrical Properties

Using the processes considered and the mixtures used, it was not possible to verify a percolation threshold, obtaining only a slight increase in the conductivity of composites. This result can be attributed to the suboptimal dispersion of fillers within the material, with the presence of multiple agglomerates of considerable size, especially in the presence of large quantities of graphite. This morphology of the material did not allow the creation of a conductive network, a necessary condition for reaching the percolation threshold. It is therefore possible to note that in general the technologies have had a certain impact on the electrical properties, due to their ability to improve the mixing or not, as can be seen from the better results of IM, the only technology that adds an additional mix after the mechanical one. The mechanical mixing process is therefore probably the most responsible for this failure to reach the percolation threshold, being the factor that most influences the final dispersion of the fillers.

Chapter 4. Discussion of the Results

Despite not having reached the percolation threshold, it is interesting to observe the influence of the fillers and the technologies used, compared to the electrical properties of the different materials, in order to have a better understanding of the possible ways to improve the results.

Going into details, the influence of the fillers over the electrical conductivity shows similar behaviour in IM and SLS, where there is a slight increase with the introduction of graphite, but the highest values are obtained using the combination of graphite and CNTs (Figure 4.13 And Figure 4.14). In Figure 4.14 the results of the two SLS mixtures are compared with an average value for pure PA12, obtained from an average of the pure PA12 values using IM and CM, since it was not considered necessary to repeat the test for the pure PA12 specimen produced with SLS.

In any case, the two technologies are not directly comparable due to the use of different quantities of fillers. Taking this into account, it is possible to note that with regard to the maximum conductivity achieved, with IM the conductivity increases by more than one order of magnitude, while using SLS it only doubles. In IM it is also interesting to note that the introduction of only 3% CNT as fillers guarantees a value more than double compared to the use of 30% of graphite.

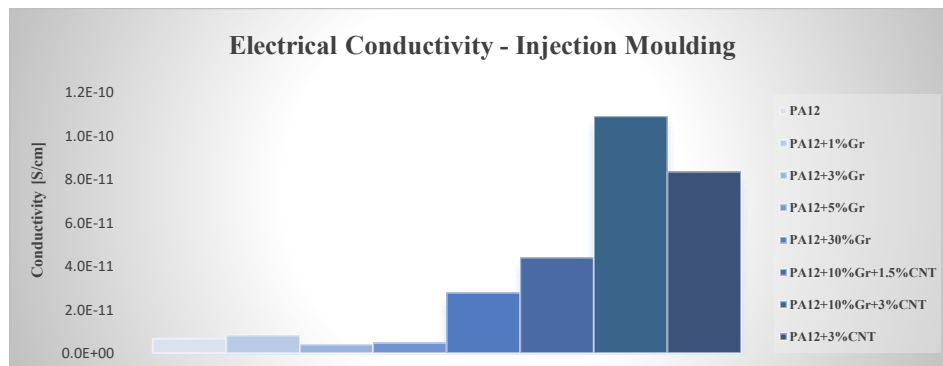


Figure 4.13 - Electrical Conductivity of IM Specimens

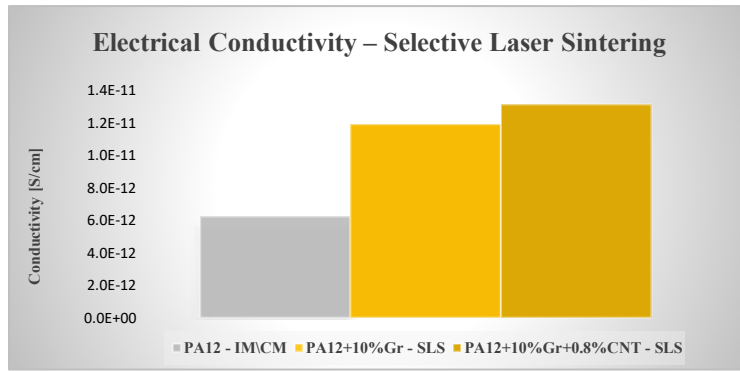


Figure 4.14 - Electrical Conductivity of SLS Specimens

As for CM, the introduction of fillers keeps the electrical conductivity equal or even worse, where this time the best solution is obtained using 30% graphite (Figure 4.15). This behaviour can be explained by observing the dispersion in the materials. In all three mixtures the dispersion is very poor, with large agglomerates of fillers, especially in the solution with 3% CNT, and this distribution makes the electron conduction more difficult.

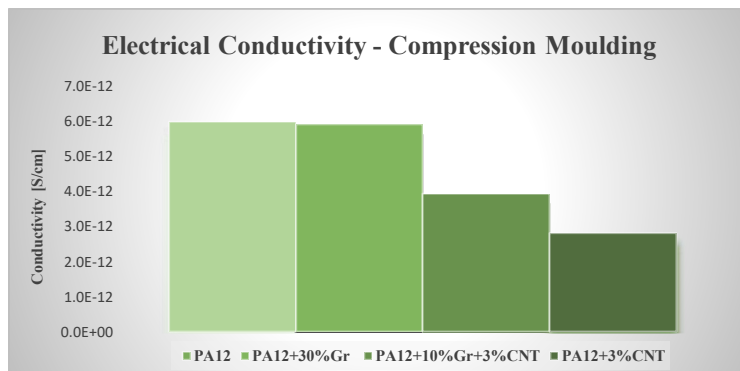


Figure 4.15 - Electrical Conductivity of CM Specimens

By assessing the impact of the technologies, as mentioned above, IM guarantees the best values with the same amount of filler (Figure 4.16). IM allows to reach values one order of magnitude higher than the use of CM.

Chapter 4. Discussion of the Results

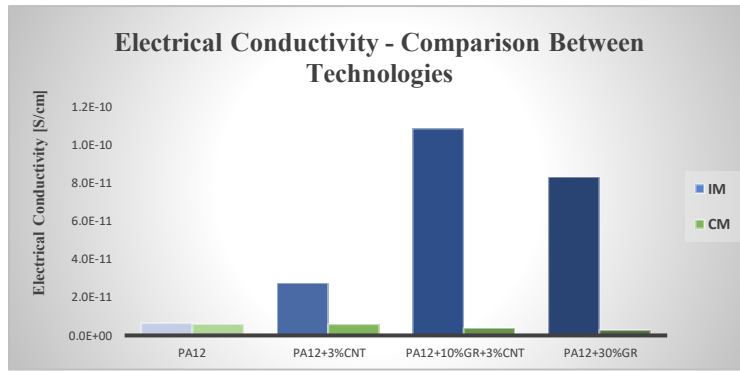


Figure 4.16 - Electrical Conductivity of Composite Specimens using IM and CM

The mixture that allows to obtain the highest electrical conductivity, and therefore the lowest electrical resistivity, is PA12 with 10% graphite and 3% CNT, which is able to reach values around 1×10^{-10} S/cm and $1 \times 10^{10} \Omega \cdot \text{cm}$ respectively (Figure 4.17). SLS obtains the best results using PA12 with 10% graphite and 0.8% CNT, reaching a value around 1×10^{-11} S/cm, therefore one order of magnitude less than with the best mixture for IM. Again, it is important to remember that these values cannot be compared directly, due to the different quantities of fillers used.

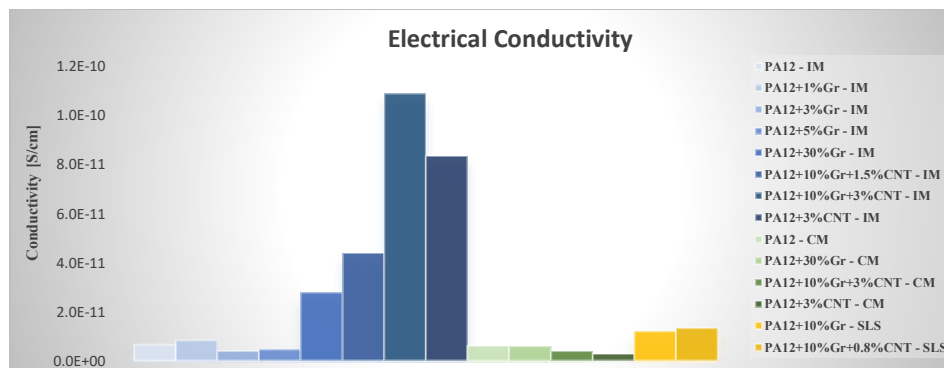


Figure 4.17 - Electrical Conductivity of the Specimens

In general, the joint effect of graphite and CNT allows to obtain the highest conductivity values, showing that their cooperation is good at least for the electrical properties. Probably their increase in performance can be further improved with a different mixing process, which would lead to an improved dispersion and therefore a better conductive network.

4.4 Thermal Properties

As happened for the electrical properties, also with reference to the thermal properties, once again the mixtures used of graphite and CNT did not bring the desired results, with the highest conductivity value around $0.4 \text{ W/m}\cdot\text{K}$. These not so good results can be explained observing the suboptimal dispersion obtained with the different mixtures, which does not allow to reach high values of thermal conductivity or a thermal conductive network. However, in this case the impact of the technologies is different from that which characterizes the electrical properties, indicating that the mixing process is probably not the main responsible for the slight increase of thermal conductivity. This is suggested by the fact that this time the technology that gives the best results is CM, which does not provide an additional mix of the material.

Even in these tests, although they have not achieved satisfactory performance such as thermal conductivity, it is interesting to analyse the performance of the properties based on the technologies and the fillers used, to understand possible ways to improve the properties obtained.

As far as details are concerned, the influence of the fillers on the thermal conductivity achieved assumes a unique trend for all three technologies, namely the highest increase using the mixture with only graphite, followed by the combination of both fillers and finally the lowest results with only CNT (Figure 4.18, Figure 4.19 and Figure 4.20). CM shows the only exception to this trend, represented by a higher conductivity value of pure PA12 compared to the values obtained with both fillers and with only CNT. This type of behaviour can be explained by still referring to the dispersion in the specimens, that is better in the solution with 30% graphite compared to the others.

Chapter 4. Discussion of the Results

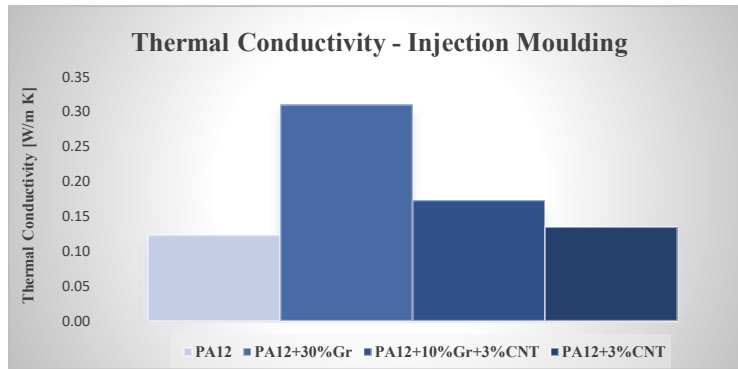


Figure 4.18 - Thermal Conductivity of IM Specimens

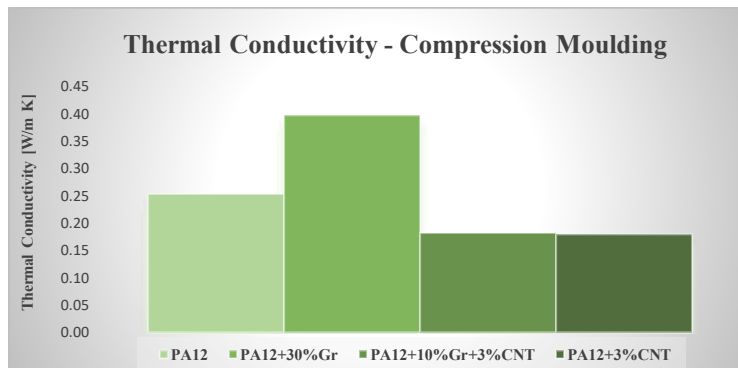


Figure 4.19 - Thermal Conductivity of CM Specimens

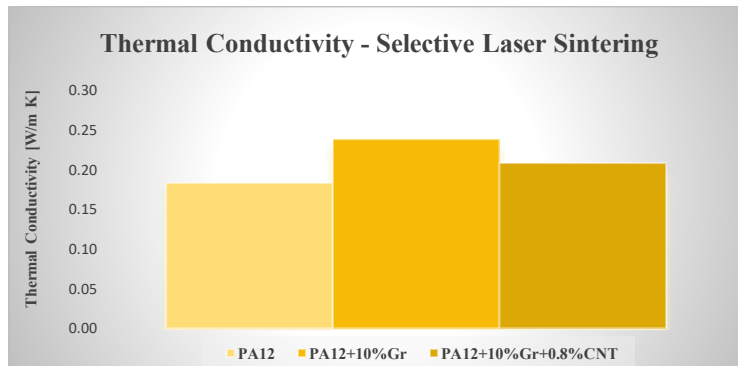


Figure 4.20 - Thermal Conductivity of SLS Specimens

The mixtures with only graphite reach much higher thermal conductivity values than pure PA12, achieving values 2.5 times higher using IM and around 1.5 times with CM and SLS.

As for the influence of technologies on the properties, CM is certainly the best technology compared to the other technologies, always guaranteeing the highest values (Figure 4.21 and Figure 4.22).

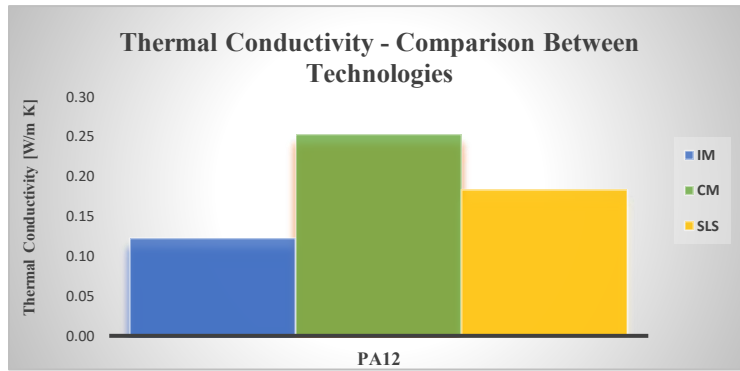


Figure 4.21 - Thermal Conductivity of pure PA12 Specimens using IM, CM and SLS

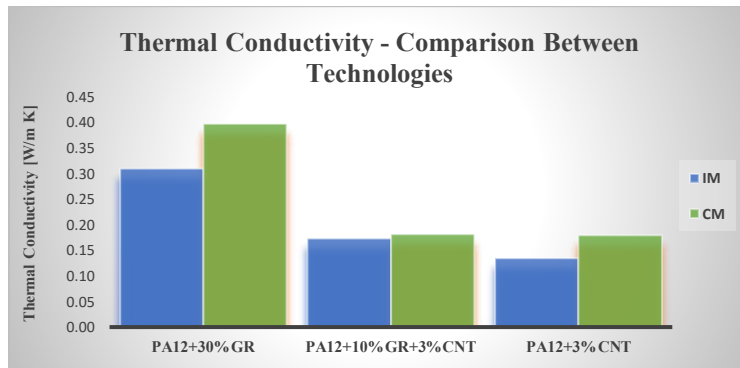


Figure 4.22 - Thermal Conductivity of Composite Specimens using IM and CM

Considering the results in general, the highest value of thermal conductivity is obtained by using the mixture with 30% graphite and CM as technology, reaching a value of about 0.4 W/m·K (Figure 4.23). As regard only SLS, the maximum value is from PA12 with 10% graphite, reaching a conductivity of around 0.24 W/m·K. It is important to consider once again the different quantities of fillers involved.

Chapter 4. Discussion of the Results

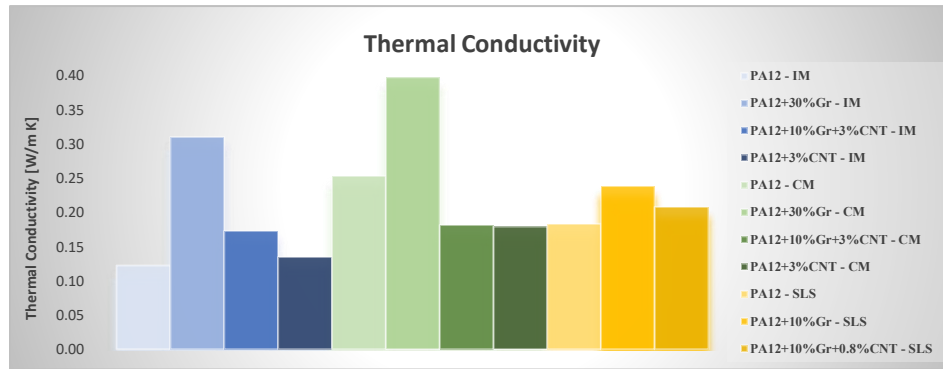


Figure 4.23 - Thermal Conductivity of the Specimens

Looking at these results, it is clear that, as regard thermal properties, the introduction of both fillers cancels the improvements of the individual fillers.

4.5 Morphology Properties

The microstructural test was conducted to study the internal morphology of the specimens, in order to understand the origin of the results from the other tests. To obtain the best possible understanding of the characteristics of the materials, in particular as regards the dispersion of the fillers which is one of the most influential parameters on the final properties, four pictures were taken with increasing magnification, in order to compare the influence of the fillers and the technologies. In the end, to complete the investigation regarding the fillers, a SEM was used to investigate the interaction between fillers and polymer. Due to the high cost of this technology, only the specimens with both fillers were studied, in order to also evaluate the interaction between the two types of fillers.

By first analysing the influence of the fillers over the morphology, starting from IM, the presence of agglomerates is evident in all composite materials (Figure 4.24). The largest agglomerates are present in the 30% graphite mixture, due to the greater quantity of fillers. Instead, the mixture with 10% graphite and 3% CNTs is the one that obtains the best dispersion, visible also through the observation that this mixture achieved the darkest colour between the three different mixtures (Figure 4.25), providing an explanation of the best results as regards the electrical properties. This characteristic, clearly not easily predicted due

to the lower concentration of fillers compared to the solution with 30% graphite, can be associated with the better mixing capacity of the IM process.

In the end, the mixture made of PA12 and 3% CNTs still shows the presence of agglomerates, even if it represents the mixture with the least amount of fillers.

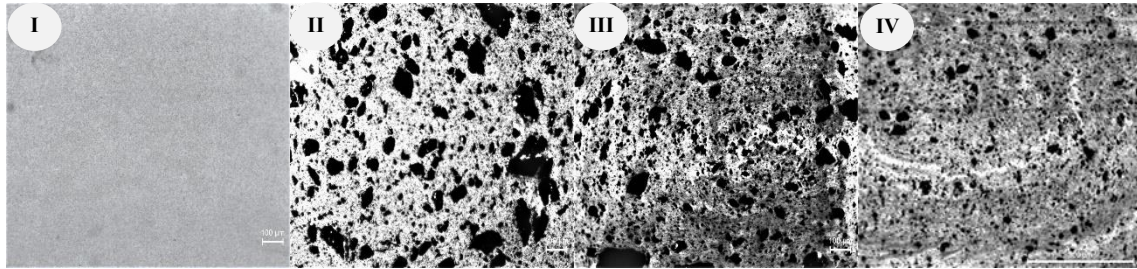


Figure 4.24 - Transversal Section of IM Specimens (10x): I) Pure PA12; II) PA12 with 30% Graphite; III) PA12 with 10% Graphite and 3% CNTs; IV) PA12 with 3% CNTs

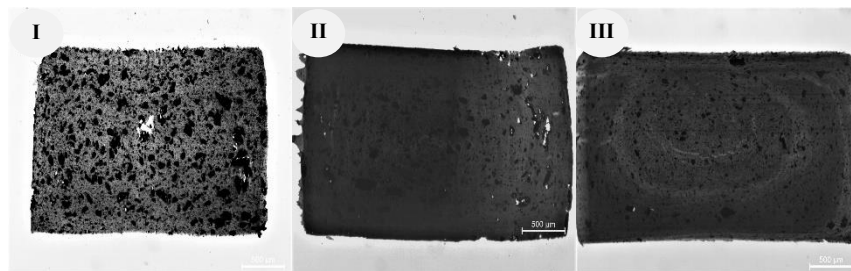


Figure 4.25 - Transversal Section of IM Specimens (4x): I) PA12 with 30% Graphite; II) PA12 with 10% Graphite and 3% CNTs; III) PA12 with 3% CNTs

As for CM, the 30% graphite mixture has the largest number of agglomerates among the mixtures (Figure 4.26). The dispersion obtained in this specific case is the best of the three different mixtures, as can be seen in Figure 4.27, due to the large amount of fillers inside the material.

An interesting element to observe this time is that the largest agglomerates are obtained when only CNTs are used, reaching a size slightly greater than that of the mixture with 30% graphite, although the amount of filler is clearly different in the two cases.

In all three mixtures it is possible to note that the presence of large agglomerates leads to a bad dispersion of the fillers, that can explain the poor results in mechanical and electrical

Chapter 4. Discussion of the Results

properties. The absence of a further mixing phase, in fact, does not allow the breakdown of the large agglomerates of fillers, not allowing to obtain a more heterogeneous material.

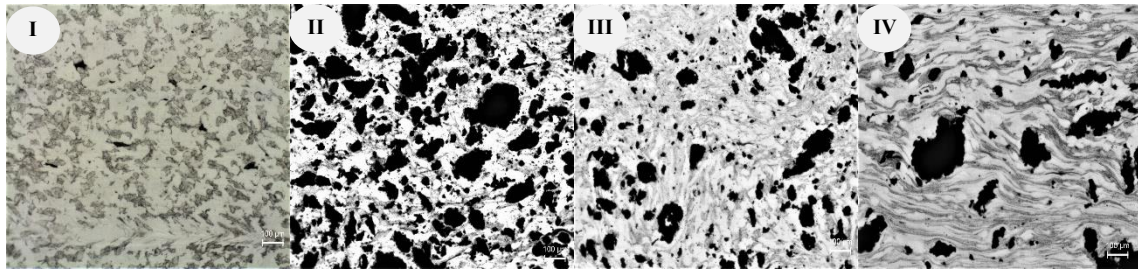


Figure 4.26 - Transversal Section of CM Specimens (10x): I) Pure PA12; II) PA12 with 30% Graphite; III) PA12 with 10% Graphite and 3% CNTs; IV) PA12 with 3% CNTs

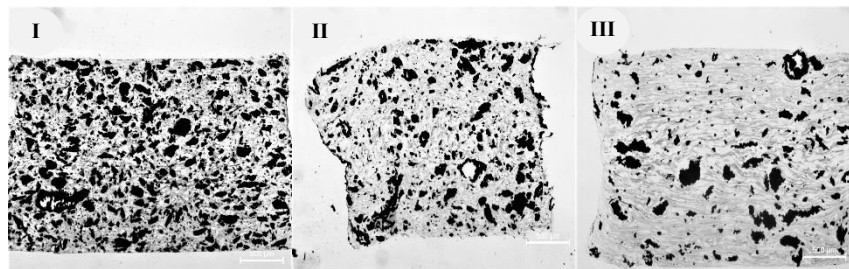


Figure 4.27 - Transversal Section of CM Specimens (4x): I) PA12 with 30% Graphite; II) PA12 with 10% Graphite and 3% CNTs; III) PA12 with 3% CNTs

As for the CM specimen with 10% graphite and 3% CNTs, it is possible to note that if the size of the agglomerates exceeds a critical size, the agglomerates are easily released from the matrix, leaving a hole in the section, as it is possible to see in Figure 4.28. This problem could lead to a deterioration in performance, especially with regard to mechanical properties.

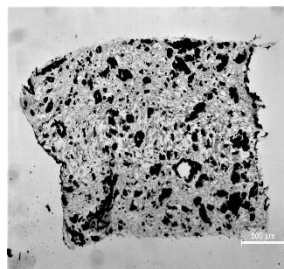


Figure 4.28 - Transversal Section of PA12 with 10% Graphite and 3% CNTs Specimen by CM (4x)

As for SLS, comparing the two different mixtures, the first observation undoubtedly concerns the great difference in the quantity of fillers present in the obtained samples, clearly visible

in Figure 4.29 and Figure 4.30. Although substantially the second mixture has only an addition of CNTs with the same amount of graphite, its sample shows a final quantity of fillers well below the initial quantity, going to highlight the impossibility of using quantities of fillers above of a critical maximum, a technical limit already known before the production of the SLS samples. This problem also highlights the need to review the results of the tests conducted on the SLS samples, taking this time into account the actual amount of fillers in the samples.

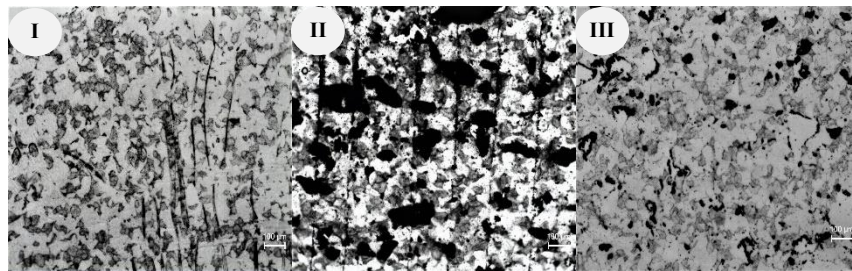


Figure 4.29 - Transversal Section of SLS Specimens (10x): I) Pure PA12; II) PA12 with 10% Graphite; III) PA12 with 10% Graphite and 0.8% CNTs

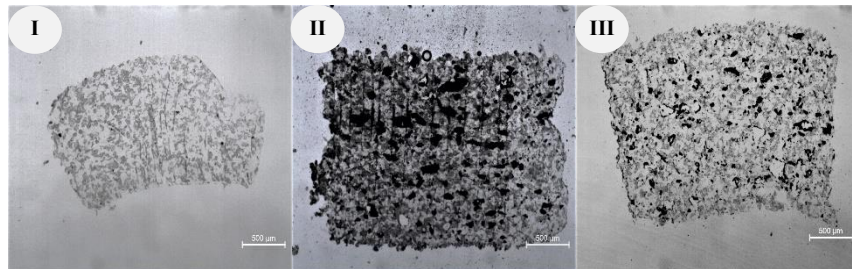


Figure 4.30 - Transversal Section of SLS Specimens (4x): I) Pure PA12; II) PA12 with 10% Graphite; III) PA12 with 10% Graphite and 0.8% CNTs

Considering the problem just highlighted, the mixture with 10% graphite obviously has the largest agglomerates and their greatest number. SLS technology, like CM, does not provide an additional mixing phase to the material, not allowing the reduction of the size of the agglomerates. Furthermore, the distribution seems to be very bad, having an area which the large agglomerates are highly concentrated and another area with a minimal quantity of them (Figure 4.30).

Chapter 4. Discussion of the Results

As for the second mixture, i.e. that with 10% graphite and the addition of 3% CNTs, the agglomerates are smaller than the 10% graphite mixture. The low number of agglomerates are due to the problem just described, i.e. the inability of the process to incorporate all the available fillers, and due to their easy release from the matrix. This second problem had already been encountered using CM, leaving some holes in the section and therefore it could cause a deterioration in the performance of the material, especially as regards the mechanical properties.

The distribution in this case seems slightly better than the previous one, but still shows some areas with less agglomerates than others.

Therefore, by analysing the influence of technologies on the morphology of pure PA12, in general it can only be observed that IM allows to achieve the best homogeneity of the material, thanks to its additional mixing process (Figure 4.31). Instead, the morphological characteristics of CM and SLS show a much greater lack of homogeneity, but in return they seem to be very similar to each other.

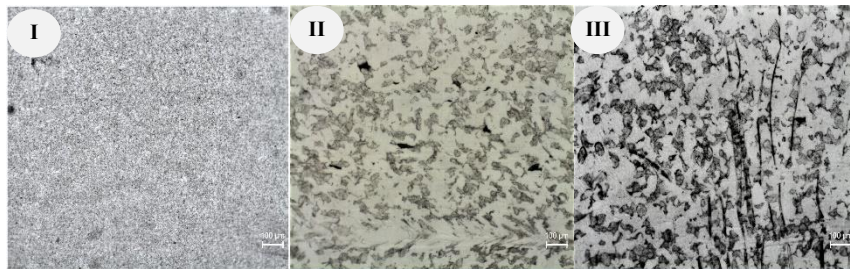


Figure 4.31 - Transversal Section of PA12 Specimens (10x): I) IM; II) CM; III) SLS

In subsequent analyses, it is appropriate to highlight the impossibility of directly comparing the influence of the three different technologies on the final morphological properties, due to the use of different quantities of fillers. Therefore, only the different influence of IM and CM has been studied in the following comparisons.

As for PA12 with 30% graphite, the mixture obtained from CM has agglomerates larger than that of IM (Figure 4.32). This observation, combined with the fact that the colour of the latter

appears much darker (Figure 4.33), indicates better dispersion using IM, once again due to the further mixing process of this process.

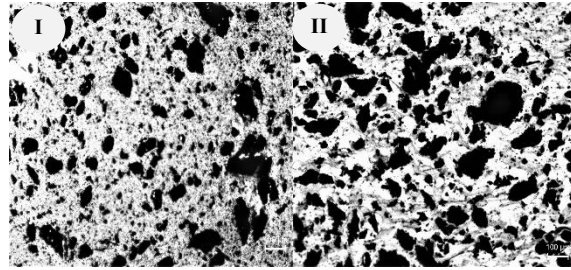


Figure 4.32 - Transversal Section of PA12 with 30% Graphite Specimens (10x): I) IM; II) CM

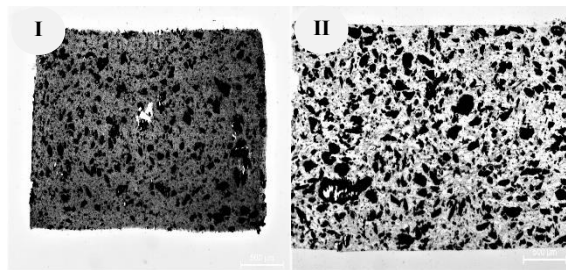


Figure 4.33 - Transversal Section of PA12 with 30% Graphite Specimens (4x): I) IM; II) CM

As for PA12 with 10% graphite and 3% CNTs, the best dispersion was again obtained using IM, a result evidenced by the smaller agglomerates and the darker colour of the material (Figure 4.34 and figure 4.35).

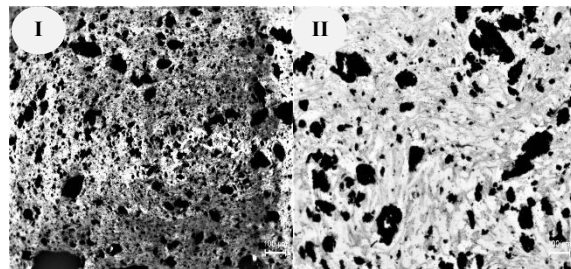


Figure 4.34 - Transversal Section of PA12 with 10% Graphite and 3% CNTs Specimens (10x): I) IM; II) CM

Chapter 4. Discussion of the Results

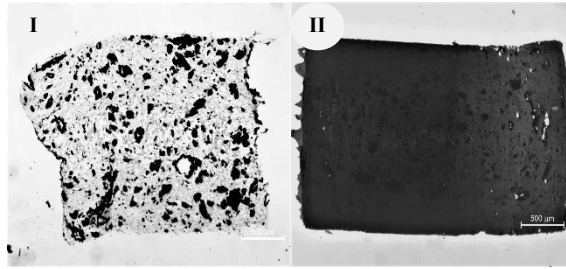


Figure 4.35 - Transversal Section of PA12 with 10% Graphite and 3% CNTs Specimens (4x): I) IM; II) CM

As for PA12 with only 3% CNTs, the CM specimens have very large agglomerates, much larger than those in IM. Furthermore, the dispersion is very different between the two technologies, showing an almost homogeneous mixture for IM and instead a very bad dispersion using CM, observation supported also by the darker colour of the IM specimen (Figure 4.36 and Figure 4.37).

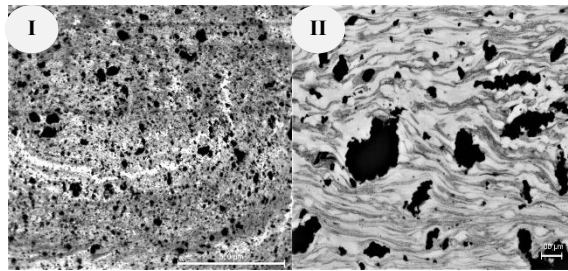


Figure 4.36 - Transversal Section of PA12 with 3% CNTs Specimens (10x): I) IM; II) CM

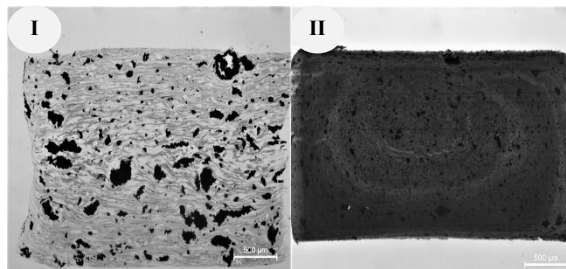


Figure 4.37 - Transversal Section of PA12 with 3% CNTs Specimens (4x): I) IM; II) CM

Using a SEM, it was possible to deepen the information on the agglomerates and the behaviour of the fillers inside the materials. Given the confirmations of this analysis to the results obtained using the microscope, and because of the cost of this investigation, it was carried out only with the mixtures containing both the fillers, in order to be able to also evaluate the interaction between them. It is important, once again, to remember the difference

between the ratios used in the IM and CM processes, equal to 10% graphite and 3% CNTs, and in the SLS process, i.e. 10% graphite and 0.8% CNTs.

The first thing that can be noticed is the remarkable porosity that characterizes the SLS specimen, totally different from IM and CM, as can be clearly seen through the numerous holes present in the section (Figure 4.38). This result was already easily foreseeable given the nature of SLS process. Porosity is also accentuated by the interaction between the polymer and the fillers, near which the porosity seems to increase.

In general, the composite seems to be more homogeneous using IM and CM than using the SLS process.

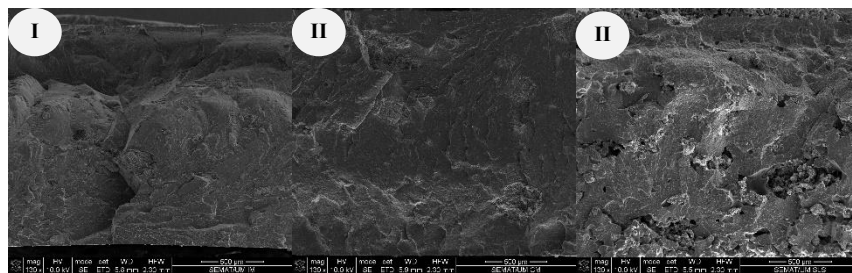


Figure 4.38 - Transversal Section of Specimens through SEM (130x): I) PA12+10%Gr+3%CNTs by IM; II) PA12+10%Gr+3%CNTs by CM; III) PA12+10%Gr+0.8%CNTs by SLS

SEM analysis confirms the results obtained with the normal microscope, showing the presence of large agglomerates in all mixtures, with the smallest found using IM and the largest ones using CM (Figure 4.39). This observation is partly able to explain the better dispersion obtained in IM compared to the other technologies.

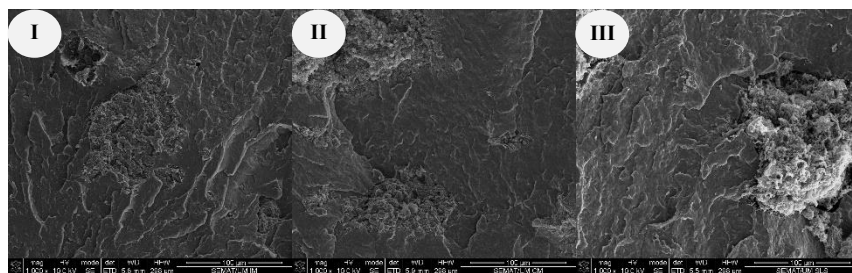


Figure 4.39 - Transversal Section of Specimens through SEM (1000x): I) PA12+10%Gr+3%CNTs by IM; II) PA12+10%Gr+3%CNTs by CM; III) PA12+10%Gr+0.8%CNTs by SLS

Chapter 4. Discussion of the Results

The better dispersion can also be explained by observing the presence of the CNTs within the three different samples (Figure 4.40). The IM specimen is the only one capable of integrating a part of the CNTs into the material, providing an excellent dispersion. This result could already be guessed by studying the final colour of the specimens, which was darker using IM, indicating a better dispersion of the fillers.

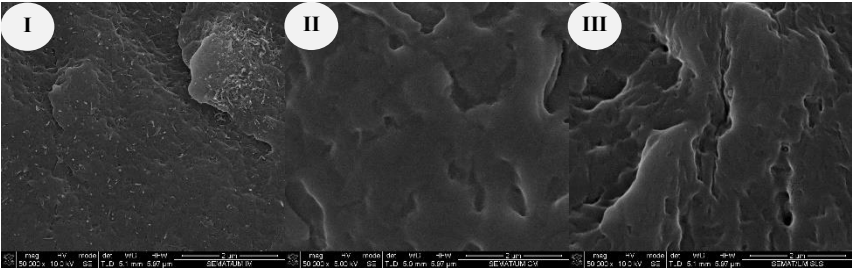


Figure 4.40 - Transversal Section of Specimens through SEM (15000x): I) PA12+10%Gr+3%CNTs by IM; II) PA12+10%Gr+3%CNTs by CM; III) PA12+10%Gr+0.8%CNTs by SLS

Chapter 5. Conclusions and Future Work

This chapter summarizes the main conclusions of this work, following up on all that has been discussed in previous chapters and highlighting some suggestions for future work.

5.1 Conclusions and Future Work

In general, the objective of producing all the specimens with any type of filler has been achieved. This objective was achieved with relative ease in the case of IM and CM, while the use of SLS entailed some greater difficulties. The problem that arose in the latter technology concerned the ability to incorporate all the quantity of fillers into the polymer matrix, especially when using both graphite and CNTs. Unlike IM and CM, in fact, a lot of reinforcement material got stuck on the roller which had the task of distributing the material on the powder bed. By comparing the images of the two SLS specimens, it seems clear that a large quantity of fillers was not incorporated when using both fillers. This is particularly interesting considering that the two solutions differ only in a small percentage of CNTs, while maintaining the same amount of graphite which is ten times greater than that of CNTs.

This problem could lead to two different interpretation: on the one hand, it highlights an evident limit of SLS, namely that of not being able to process composites with a quantity of fillers beyond a certain threshold. A detailed study of this specific threshold is still missing in literature and it can certainly be an interesting research for future applications of composite materials. This could also be associate with a contemporary study on the influence of the filler size on the filler threshold, leading to the possibility of knowing in advance which could be the best type of filler to add to the polymer matrix based on the size and the corresponding limit.

On the other hand, the problem could arise from the interaction between graphite and CNTs, with consequent even larger agglomerates, which would become too large for the layer thickness. This hypothesis should also be studied in more detail in order to understand the exact interaction dynamics of the two fillers inside the SLS chamber. A better understanding could lead to the choice of another material to be associated with the graphite or to the modification of one of the two fillers to limit the agglomerates as much as possible, leading to better final properties of the composite.

Considering the properties studied with the various tests and remembering once again the differences in the ratios between IM/CM and SLS, in general the results obtained are not entirely satisfactory, especially from the point of view of the search for a new improved

material to be used in SLS. Both electrical and thermal conductivity show mediocre increases with any filler, or even a worsening of properties in the case of CM. In no case was the percolation threshold reached, demonstrating an insufficient dispersion of the fillers inside the composites, the main factor contributing to the electrical conductivity, while the thermal conductivity did not reach any considerable results, with the result that the composites remain both electrically and thermally insulated. The mechanical test results show a substantial difference between the IM specimens and the CM/SLS specimens, i.e. a general increase in properties with the use of the first technology and a general decrease with the others, with the only exception of elongation at break which decreases in any case [77].

However, it should be remembered that the real presence of fillers within the specimens obtained from SLS is certainly far from the theoretical value, just as that this theoretical value is in any case lower than that used with the other two technologies. The actual ability of the fillers to improve is therefore difficult to interpret and would require further investigation.

Although it has not been possible considerably improve the properties of the composites, it is possible to note that the results show a real influence of the fillers on the properties of the various mixtures. Graphite alone is certainly the best filler to add if the objective is a general improvement in thermal and some mechanical properties, while the addition of both graphite and CNTs or only CNTs leads to a general improvement in electrical properties.

In the case of graphite, the results can be explained considering that the total quantity of fillers is about three time greater than that with both fillers, and this can explain the higher mechanical properties, related to the transfer of the load from the matrix to the reinforcement, and the higher thermal properties, since the resulting thermal conductivity increases with increasing load of highly conductive fillers. The inefficiency shown by CNTs on thermal conductivity is caused by the simple incorporation of this type of fillers into the matrix, a fact already known in the literature, which significantly reduces the high intrinsic thermal conductivity of CNTs [77].

The case of CNTs or both fillers would require further investigation to investigate the underlying causes of the greater conductivity shown by the use of these two solutions. The most probable hypotheses are that the interaction of the two fillers, or the use of CNTs only,

Chapter 5. Conclusions and Future Work

can lead to better dispersion, which is the key factor capable of increasing the general conductivity of the matrix, or that the high intrinsic electrical conductivity of CNTs can contribute much more than a much greater amount of graphite. It is also important to note that a large amount of graphite within the material leads to larger agglomerates that worsens conduction, which may partially explain the lower conductivity. A better understanding of the reasons behind these electrical results could allow the creation of a conductive network and therefore make the composite conductive [77][78].

Going into the details of the electrical properties, the introduction of the fillers in the SLS and CM specimens shows only a slight increase in conductivity or even a worsening, unlike IM in which the increment appears much greater. By evaluating the difference in the two results and considering the literature, it is possible to attribute the greater electrical conductivity in IM to the better mixing, and therefore to the better dispersion, that this technology is able to provide to the composite through the internal mixing of the process itself [78].

Also in general, IM seems to be the technology capable of guaranteeing the best properties or the greatest improvements in all the properties studied. Considering the main differences and similarities between the three processes, it seems that the influence of mixing, and therefore of dispersion, has once again shown to play an important role on the final properties of the specimens, as usually confirmed in literature [78][79].

From this study it seems that a better mixing process could significantly improve the properties of the different mixtures, therefore an interesting research would concern the influence of the initial mixing process on the final properties. A better mixing should allow for better dispersion, which in turn should significantly improve not only electrical properties, but also mechanical and thermal properties. This improved dispersion would allow SLS composites to approach the properties obtained with the IM process, increasing their use in different fields of application [77].

In addition to dispersion, the second important factor on which it would be possible to work is the functionalization of the fillers. Functionalizing the fillers, i.e. changing the surface properties, should not only significantly improve the dispersion of fillers, but should also

significantly improve the strength of the interface between the fillers and the matrix, thus leading to a significant increase in the resulting properties of the composite, as shown in many occasions in literature [12][42][43][44][80][81].

Both the fillers used in this work can be modified to increase the interfacial adhesion with the polymer to which they will be added. In the case of graphite, some examples that can be obtained through the modification of this type of filler are graphite oxide (GO), expanded graphite (EG) and graphite intercalated compounds (GICs) [25][81].

As for CNTs, it would be possible to functionalize the inherently nature of CNTs using two main approaches, namely chemical and physical functionalization. Some examples of techniques belonging to the first type are fluorination, cycloaddition, chlorination and hydrogenation, while polymer wrapping, surfactant adsorption and endohedral method belong to physical functionalization. Surface functionalization would help stabilize the dispersion within the composite, preventing re-aggregation and leading to a better coupling of CNTs with the polymer matrix [42][43][82].

Although studies on the changes mentioned above have already been conducted, their influence on the PA specimens produced by SLS is still unknown, as well as their mutual influence over the properties of this process. The increase in adhesion should in any case further improve the resulting properties of the composites, also allowing in this case to approach the properties obtained with the IM process.

Finally, following the good results of graphite and CNTs in influencing the mechanical, thermal and electrical properties, future works could focus on other carbon-based fillers to further improve the resulting properties of the SLS composites. Some interesting fillers in this case could be carbon black (CB), carbon nanofibers (CNFs), graphite nanoplatelets (GNPs) and mainly graphene with its derivatives. The latter in particular have seen growing interest in recent years due to their promising properties, but their application in the field of SLS is still limited [5][25][77][79][83][84].

Chapter 5. Conclusions and Future Work

References

- [1] ISO International Organization for Standardization, ISO/ASTM 52900 Additive manufacturing - General principles - Terminology, 2018.
- [2] Homepage University of Texas, *Selective Laser Sintering, Birth of an Industry*, Accessed 17 November 2019, <<http://www.me.utexas.edu/news/news/selective-laser-sintering-birth-of-an-industry>>.
- [3] A. C. F. Lopes, "Study and evaluation of different combinations of virgin and processed PA material for Selective Laser Sintering technology", University of Minho (Master's Thesis), July 2018.
- [4] I. Gibson, D. W. Rosen, B. Stucker, "Additive Manufacturing Technologies: Rapid Prototyping to Direct Digital Manufacturing", *Springer*, pp. 103-105, 138-140, April 2010.
- [5] M. Schmid, "Laser Sintering with Plastics: Technology, Processes, and Materials", *Hanser Publications*, pp. 39-51, 65-66, 71-78, 125-131, 134, 151, September 2018.
- [6] D. T. Pham, S. S. Dimov, "Rapid Manufacturing: The Technologies and Applications of Rapid Prototyping and Rapid Tooling", *Springer*, pp. 55-57, April 2001.
- [7] P. K. Venuvinod, W. Ma, "Rapid Prototyping: Laser-based and Other Technologies", *Springer Science & Business Media*, pp. 247-249, April 2013.
- [8] K. G. Cooper, "Rapid Prototyping Technology: Selection and Application", *Marcel Dekker*, pp. 128, January 2001.
- [9] EOS, *Additive Manufacturing, Laser-Sintering and industrial 3D printing - Benefits and Functional Principle*, Accessed 22 November 2019, <https://www.eos.info/additive_manufacturing/for_technology_interested>.
- [10] A. F. A. Becker, "Characterization and Prediction of SLS Processability of Polymer Powders with respect to Powder Flow and Part Warpage", pp. 21, 2016.
- [11] B. Caulfield, P. E. McHugh, S. Lohfeld, "Dependence of mechanical properties of polyamide components on build parameters in the SLS process", 2006.
- [12] M. Schmid, A. Amado, K. Wegener, "Polymer Powders for Selective Laser Sintering (SLS)", *AIP Publishing LLC.*, May 2015.

- [13] U.S. patent #133229, November 1872.
- [14] D. M. Bryce, "Plastic Injection Molding: manufacturing process fundamentals", *Society of Manufacturing Engineers*, pp. 29-55, 98-105, April 1996.
- [15] G. Pötsch, W. Michaeli, "Injection Molding: An Introduction", *Hanser Publishers*, pp. 1-12, 57, 110-111, 118-122, 170-172, August 1995.
- [16] T. A. Osswald, G. Mendes, "Material Science of Polymers for Engineers", *Hanser Publishers*, pp. 206-215, 113-116, September 2012.
- [17] Xcentric Mold & Engineering 1996, "Injection Molding Process", Accessed 10 October 2019, <<https://www.xcentricmold.com/injection-molding-process/>>.
- [18] D. O. Kazmer, "Injection Mold Design Engineering", *Hanser Publishers*, pp. 2-3, 78-80, 246, 302, 311, 325, 475, 496, March 2016.
- [19] Polyplastic Co., "The Outline of Injection Molding", Accessed 15 October 2019, <<https://www.polyplastics.com/en/support/mold/outline/>>.
- [20] D. V. Rosato, D. V. Rosato, M. G. Rosato, "Injection Molding Handbook", Third Edition, *Kluwer Academic Publisher*, pp. 4-8, 32, 73, 110-111, 144, 149, 183, 203, 260-262, 273, 280-282, 401, 418-446, 498-521, 537-541, 571, 579, 591-593, 627-628, 634-642, 857, 973-975, 2000.
- [21] D. M. Bryce, "Plastic Injection Molding: material selection and product design fundamentals", *Society of Manufacturing Engineers*, pp. 154, April 1996.
- [22] R. Kerkstra, S. Brammer, "Injection Molding Advanced Troubleshooting Guide", *Carl Hanser Verlag*, pp. 81-90, 106, 125, 165-167, 182-185, 265-267, 281-296, 348, 377-393, 403, 408, 434, 464, 2018.
- [23] L. Xie, L. Shen, B. Jiang, "Modelling and Simulation for Micro Injection Molding Process", *IntechOpen*, July 2011.
- [24] M. R. Kamal, A. Isayev, S. Liu, "Injection Molding Technology and Fundamentals", *Hanser Publishers*, pp. 10-13, 20-24, 51-60, 88, 106, 128-131, 443, 135, 139, 703-710, 859-884, 2009.
- [25] D. V. Rosato, "Plastic Processing Data Handbook", *Chapman & Hall*, pp. 415-423, 1997.

- [26] M. Kutz, "Applied Plastics Engineering Handbook: Processing, Materials and Applications", *Elsevier Inc.*, pp. 61, 291-320, 523-526, 2017.
- [27] D. V. Rosato, D. V. Rosato, M. V. Rosato, "Plastic Product Material and Process Selection Handbook", *Elsevier Science & Technology Books*, pp. 439-453, 2004.
- [28] S. Kalpakjian, S. R. Schmid, "Manufacturing Engineering and Technology", *Pearson*, pp. 503-504, March 2013.
- [29] R. F. Gibson, "Principles Of Composite Material Mechanics", *4th ed CRC Press*, pp. 1-13, 231, 271-272, 502-505, 2016.
- [30] J. McLoughlin, T. Sabir, "High-Performance Apparel: Materials, Development, and Applications", *Woodhead Publishing*, pp. 206, 386, 579-586, 2018.
- [31] S. G. Advani, K. Hsiao, "Manufacturing techniques for polymer matrix composites (PMCs)", *Woodhead Publishing*, pp. 1-5, 15-61, 95-96, 101-105, 108-115, 260, 2012.
- [32] N. Ramdani, "Polymer and Ceramic Composite Material: Emergent Properties and Applications", *CRC Press*, pp. 1-7, 115-116, 2019.
- [33] S. Yuan, F. Shen, C. K. Chua, K. Zhou, "Polymeric composites for powder-based additive manufacturing: Materials and applications", *Elsevier*, November 2018.
- [34] K. K. Chawla, "Composite Materials: Science and Engineering", *4th ed Springer*, pp.139-140, 297, 365-366, 2019.
- [35] J.-P. Kruth, G. Levy, R. Schindel, T. Craeghs, E. Yasa, "Consolidation of Polymer Powders by Selective Laser Sintering", *Elsevier*, 2008.
- [36] V. Francis, P. K. Jain, "Advances in nanocomposite material for additive manufacturing", *Int. J. Rapid Manufacturing*, Vol. 5, Nos. 3/4, pp.215–233, 2015.
- [37] S. Kumar, J.-P. Kruth, "Composites by rapid prototyping technology", *Elsevier*, August 2009.
- [38] A. C. de Leon, Q. Chen, N. B. Palaganas, J. O. Palaganas, J. Manapat, R. C. Advincula, "High performance polymer nanocomposites for additive manufacturing applications", *Elsevier*, April 2016.
- [39] P. Parandoush, D. Lin, "A review on additive manufacturing of polymer-fiber composites", *Elsevier*, September 2017.

- [40] M. Brandt, "Laser Additive Manufacturing: Materials, Design, Technologies, and Applications", *Woodhead Publishing*, pp. 205-235, 2017.
- [41] J. H. Koo, S. Lao, W. Ho, K. Nguyen, J. Cheng, L. Pilato, G. Wissler, M. Ervin, "Polyamide nanocomposites for selective laser sintering", *17th Solid Freeform Fabrication Symposium*, pp. 392-409, 2006.
- [42] R. D. Goodridge, M. L. Shofner, R. J. M. Hague, M. McClelland, M. R. Schlea, R. B. Johnson, C. J. Tuck, "Processing of a Polyamide-12/carbon nanofibre composite by laser sintering", *Elsevier*, October 2010.
- [43] J. Cheng, S. Lao, K. Nguyen, W. Ho, A. Cummings, J. Koo, "SLS Processing Studies of Nylon 11 Nanocomposites", *16th Solid Freeform Fabrication Symposium*, 2005.
- [44] Y. Wang, D. Rouholamin, R. Davies, O. R. Ghita, "Powder Characteristics, Microstructure and Properties of Graphite Platelet Reinforced Poly Ether Ether Ketone composites in High Temperature Laser Sintering (HT-LS)", *Elsevier*, December 2015.
- [45] X. Wang, M. Jiang, Z. Zhou, J. Gou, D. Hui, "3D printing of polymer matrix composites: A review and prospective", *Elsevier*, November 2016.
- [46] J. C. Nelson, N. K. Vail, J. W. Barlow, "Laser Sintering Model for Composite Materials", *1993 International Solid Freeform Fabrication Symposium*, 1993.
- [47] V. K. Thakur, M. K. Thakur, R. K. Gupta, "Hybrid Polymer Composite Materials: Processing", *Woodhead Publishing*, pp. 7-11, 145-147, 199, 219-225, 257, 312-313, 2017.
- [48] S. M. Lee, L. Nicolais, A. Borzacchiello, "Encyclopedia of Composites", *2nd ed Wiley*, pp. 128-139, 213-230, 366, 847, 1428, 1431-1437, 1542, 2039, 2153, 2536, 2683-2717, 2959, 3079, May 2012.
- [49] H. C. H. Ho, W. L. Cheung, I. Gibson, "Effects of graphite powder on the laser sintering behaviour of polycarbonate", *Rapid Prototyping Journal*, 2002.
- [50] T. Navrátil, J. Barek, M. Kopanica, "Anodic stripping voltammetry using graphite composite solid electrode", *Collect. Czech. Chem. Commun.*, 2009.
- [51] S. A. Martins, J. M. L. Reis, H. S. C. Mattos, "Mechanical and electric behavior of epoxy/graphite composite reinforced with carbon fiber for applications in fuel cell components", *Conf.: Congr. Bras. de Engen. e Ciência dos Materiais*, November 2014.

[52] R. Sengupta, M. Bhattacharya, S. Bandyopadhyay, A. K. Bhowmick, "A review on the mechanical and electrical properties of graphite and modified graphite reinforced polymer composites", *Elsevier*, November 2010.

[53] V. Panwar, R. M. Mehra, "Analysis of Electrical, Dielectric, and Electromagnetic Interference Shielding Behavior of Graphite Filled High Density Polyethylene Composites", *Polymer Engineering & Science*, 2008.

[54] X.-S. Yi, Y.-H. Song, Q. Zheng, "A preliminary study on mechanical-electrical behavior of graphite powder-filled high-density polyethylene composites", *Journal of Applied Polymer Science*, July 2000.

[55] I. Krupa, I. Novák, I. Chodák, "Electrically and thermally conductive polyethylene/graphite composites and their mechanical properties", *Elsevier*, July 2004.

[56] P. Zhang, D. Cao, S. Cui, " Resistivity-Temperature Behavior and Morphology of Low Density Polyethylene/Graphite Powder/Graphene Composites", *Polymer Composites*, Dec. 2013.

[57] X. Wu, J. Qiu, P. Liu, E. Sakai, "Preparation and characterization of polyamide composites with modified graphite powders", *Journal of Polymer Research*, September 2013.

[58] K. Scully, R. Bissessur, "Decomposition kinetics of nylon-6/graphite and nylon-6/graphite oxide composites", *Elsevier*, February 2009.

[59] H. Miyanaji, J. M. Akbar, L. Yang, " Fabrication and characterization of Graphite/Nylon 12 composite via binder Jetting additive manufacturing process", *Conf.: 28th Annual Intern. SFF Symposium*, August 2017.

[60] K. Wakabayashi, C. Pierre, D. A. Dikin, R. S. Ruoff, T. Ramanatha, L. C. Brinson, J. M. Torkelson, "Polymer-Graphite Nanocomposites: Effective Dispersion and Major Property Enhancement via Solid-State Shear Pulverization", *Macromolecules*, February 2008.

[61] R. M. Morsy, M. N. Ismaiel, A. A. Yehia, "Conductivity Studies on Acrylonitrile Butadiene Rubber Loaded with different types of Carbon Blacks", *International Journal of Materials, Methods and Technologies*, May 2013.

- [62] M. N. Ismail, A. I. Khalaf, "Styrene–Butadiene Rubber/Graphite Powder Composites: Rheometrical, Physicomechanical, and Morphological Properties", *Journal of Applied Polymer Science*, April 2011.
- [63] M. H. Abd-El Salam, G. M. Elkomy, H. Osman, M. R. Nagy, F. El-Sayed, " Structure–electrical conductivity of polyvinylidene fluoride/graphite composites", *Journal of Reinforced Plastics and Composites*, October 2012.
- [64] C.-S. Wang, E. W. Blaha, "Graphite Powder-Polyphenylene Mixtures and Composites", *US Patent 3,971,748*, July 1976.
- [65] W.-P. Shih, L.-C. Tsao, C.-W. Lee, M.-Y. Cheng, C. Chang, Y.-J. Yang, K.-C. Fan, "Flexible Temperature Sensor Array Based on a Graphite-Polydimethylsiloxane Composite", *Sensors*, April 2010.
- [66] V. K. Srivastava, J. P. Pathak, "Friction and wear properties of bushing bearing of graphite filled short glass fibre composites in dry sliding", *Elsevier*, November 1995.
- [67] X.-R. Zhang, X.-Q. Pei, Q.-H. Wang, "Friction and wear studies of polyimide composites filled with short carbon fibers and graphite and micro SiO₂", *Elsevier*, April 2009.
- [68] W. Wang, Y. Zhu, S. Liao, J. Li, "Carbon Nanotubes Reinforced Composites for Biomedical Applications", *Hindawi Publishing Corporation*, February 2014.
- [69] V. Choudhary, A. Gupta, "Polymer/Carbon Nanotube Nanocomposites", *Polymer/Carbon Nanotube Nanocomposites*, August 2011.
- [70] J. Chen, L. Yan, Q. Song, D. Xu, "Interfacial characteristics of carbon nanotube-polymer composites: A review", *Elsevier*, August 2018.
- [71] R. Andrews, M.C. Weisenberger, "Carbon nanotube polymer composites", *Elsevier*, October 2003.
- [72] S. R. Athreya, K. Kalaitzidou, S. Das, " Processing and characterization of a carbon black-filled electrically conductive Nylon-12 nanocomposite produced by selective laser sintering", *Elsevier*, December 2009.
- [73] R. Asmatulu, W. S. Khan, R. J. Reddy, M. Ceylan, "Synthesis and Analysis of Injection-Molded Nanocomposites of Recycled High-Density Polyethylene Incorporated With Graphene Nanoflakes", *Society of Plastics Engineers*, May 2014.

- [74] ISO International Organization for Standardization, ISO 527-2 Plastics - Determination of Tensile Properties, 1996.
- [75] J. Bai, R. D. Goodridge, R. J. M. Hague, M. Song, M. Okamoto " Influence of carbon nanotubes on the rheology and dynamic mechanical properties of polyamide-12 for laser sintering", *Elsevier Ltd*, March 2014.
- [76] V. Datsyuk, S. Trotsenko, S. Reich, "Carbon-nanotube–polymer nanofibers with high thermal conductivity", *Elsevier Ltd*, September 2012.
- [77] N. Burger, A. Laachachi, M. Ferriol, M. Lutz, V. Toniazzo, D. Ruch, "Review of thermal conductivity in composites: Mechanisms, parameters and theory", *Elsevier*, May 2016.
- [78] A. Al-Dahawi, O. Öztürk, F. Emami, G. Yildirim, M. Şahmaran, "Effect of mixing methods on the electrical properties of cementitious composites incorporating different carbon-based materials", *Elsevier*, December 2015.
- [79] S. Lee, Y.-P. Jeon, "Effects of Mixing on Electrical Properties of Carbon Nanofiber and Polymer Composites", *Journal of Applied Polymer Science*, March 2009.
- [80] P.-C. Ma, N. A. Siddiqui, G. Marom, J.-K. Kim, "Dispersion and functionalization of carbon nanotubes for polymer-based nanocomposites: A review", *Elsevier*, July 2010.
- [81] M. Rahmat, P. Hubert, "Carbon nanotube–polymer interactions in nanocomposites: A review", *Elsevier*, October 2011.
- [82] D. D. L. Chung, "A review of exfoliated graphite", *Springer*, July 2015.
- [83] A. Borenstein, O. Hanna, R. Attias, S. Luski, T. Brousse, D. Aurbach, "Carbon-based composite materials for supercapacitor electrodes: a review", *J. Mater. Chem. A*, May 2017.
- [84] J. Wang, X. Jin, C. Li, W. Wang, H. Wu, S. Guo, "Graphene and graphene derivatives toughening polymers: Toward high toughness and strength", *Elsevier*, March 2019.

Sommario

Compositi a base di PA12 con grafite e MWCNT prodotti tramite SLS, Stampaggio ad Iniezione e Stampaggio a Compressione: analisi delle prestazioni

La continua crescita della Sinterizzazione Laser Selettiva (SLS) è strettamente legata allo sviluppo di materiali sempre nuovi, in grado di avvicinarsi il più possibile ai risultati ottenuti con le tecnologie di produzione tradizionali come lo Stampaggio ad Iniezione (IM) e lo stampaggio a compressione (CM).

Pertanto, questo studio si è focalizzato sullo studio dell'influenza della grafite e dei nanotubi di carbonio (CNT) in un composito a matrice polimerica (PMC), in cui la poliammide 12 (PA12) è stata utilizzata come matrice, producendo campioni con tre diverse tecnologie, vale a dire SLS, IM e CM. I principali rapporti studiati sono stati PA12 con 30% di grafite, PA12 con 10% di grafite e 3% di CNT, PA12 con 3% di CNT, PA12 con 10% di grafite, PA12 con 0,8% di CNT. I campioni ottenuti sono stati quindi sottoposti a test meccanici, elettrici, termici e morfologici.

I risultati di questa ricerca hanno mostrato una reale influenza della grafite e dei nanotubi sulle proprietà finali, sebbene la conducibilità elettrica e termica abbia subito scarsi miglioramenti, non permettendo di ottenere materiali sufficientemente conduttivi. Nonostante ciò, la grafite sembra essere il miglior filler da aggiungere se gli obiettivi sono le proprietà meccaniche e termiche, mentre entrambi i filler, o solo i CNT, mostrano un maggiore aumento delle proprietà elettriche. La dispersione sembra essere la principale responsabile di questi risultati, alla luce dei migliori risultati forniti dall'IM e dalla sua miscelazione intrinseca.